Applied Geochemistry 116 (2020) 104561

Contents lists available at ScienceDirect

Applied Geochemistry

journal homepage: http://www.elsevier.com/locate/apgeochem

Plutonium oxidation states in the Waste Isolation Pilot Plant repository

J.A. Schramke [a,*], E.F.U. Santillan [b], R.T. Peake [b]

[a] SC&A Inc, 2200 Wilson Blvd, Suite 300, Arlington, VA, 22201, USA
[b] U.S. Environmental Protection Agency, Office of Air and Radiation, USA

ARTICLE INFO

Handling editor: Prof. M. Kersten

Keywords:
Plutonium
Oxidation states
Redox
Solubility
Speciation
Waste disposal
Transuranic

ABSTRACT

The Waste Isolation Pilot Plant (WIPP), a deep geologic repository located 660 m underground in bedded salt, is designed to isolate U.S. defense-related transuranic waste from the accessible environment. Plutonium isotopes are the most important radionuclides in WIPP waste. Plutonium solubility in WIPP brines (ionic strengths from 5.3 to 7.4) is strongly dependent on its oxidation state, with much lower solubilities associated with Pu(III) and Pu(IV) than with the higher Pu(V) and Pu(VI) oxidation states. The large quantity of metallic iron in WIPP waste and waste containers is expected to undergo anoxic corrosion, producing strongly reducing conditions and high hydrogen gas pressures after repository closure and brine intrusion. Because reducing conditions will prevail in the WIPP repository, the most important long-term oxidation states will be Pu(III) and Pu(IV). We performed a literature review to evaluate the effects of WIPP chemical and physical processes on dissolved (not colloidal) plutonium oxidation states that included reactions with reducing agents such as iron solids and aqueous species and radiolysis of solids and aqueous species. The results of this review indicate that equilibrium between Pu(III) solids and aqueous species will control dissolved plutonium concentrations in WIPP brines. We also performed geochemical modeling calculations using the ThermoChimie database to support this assessment of plutonium oxidation states in the long-term WIPP repository. Control of plutonium solubilities by Pu(III) solid instead of Pu (IV) solid may lead to higher predicted plutonium concentrations in brines potentially released to the ground surface by an inadvertent drilling intrusion into the long-term WIPP repository. The results of this study demonstrate that Pu(III) solid solubilities provide a reasonable upper bound for dissolved plutonium concentrations in WIPP brines.

1. Introduction

Disposal of radioactive waste in deep geologic repositories has been proposed at a number of sites, including Forsmark in Sweden, Onkalo in Finland, Cigéo in France, and Gorleben in Germany. The host rock at these sites varies from crystalline granitic rock to clays to bedded or domal salt (Swedin, 2019). Belgium, Canada, the Czech Republic, Japan, Switzerland, and the United Kingdom are also considering deep geologic repositories. Repository depth, host rock and hydrology, waste form, and other factors such as engineered barriers will influence the physical and chemical conditions in each deep geologic repository, and these conditions will affect actinide geochemistry. Interactions between the physical and chemical processes in a deep geologic repository may affect the redox status of radionuclides such as plutonium, which in turn affects its aqueous solubility, intrinsic colloid formation, and potential releases from the repository. Currently, the only operating deep geologic repository is the Waste Isolation Pilot Plant (WIPP) located near Carlsbad, New Mexico, providing a model for assessing actinide chemistry during long-term disposal.

As authorized by the WIPP Land Withdrawal Act (U.S. Congress, 1996), the U.S. Department of Energy (DOE) manages the repository, with regulatory oversight of radioactive material provided by the U.S. Environmental Protection Agency (EPA). EPA reviews WIPP's compliance with waste disposal standards every five years by evaluating a compliance recertification application prepared by DOE. EPA first certified WIPP in 1998 and waste emplacement began in 1999. The total capacity of WIPP is 175,564 m^3 of transuranic (TRU) waste (U.S. Congress, 1996).

The WIPP repository is designed to isolate defense-related TRU waste from the accessible environment. The repository is 660 m underground in the Salado Formation, a massive bedded salt formation composed primarily of halite [NaCl(s)], with smaller amounts of anhydrite [$CaSO_4$(s)] and clay (DOE, 2014). Bedded salt was chosen for the repository location because the ductile, highly impermeable salt will

* Corresponding author.
E-mail address: ja_schramke@enchemica.com (J.A. Schramke).

https://doi.org/10.1016/j.apgeochem.2020.104561
Received 27 August 2019; Received in revised form 30 January 2020; Accepted 27 February 2020
Available online 4 March 2020
0883-2927/© 2020 The Authors. Published by Elsevier Ltd. This is an open access article under the CC BY-NC-ND license (http://creativecommons.org/licenses/by-nc-nd/4.0/).

Table 1
WIPP brine compositions.

Component	Salado Brine (GWB)	Salado Brine (GWB) After Reaction with Waste, Brucite, Hydromagnesite, Halite and Anhydrite	Castile Brine (ERDA-6)	Castile Brine (ERDA-6) After Reaction with Waste, Brucite, Hydromagnesite, Halite and Anhydrite
Boron	0.158	0.186	0.063	0.0623
Calcium	0.014	0.0111	0.012	0.0116
Potassium	0.467	0.550	0.097	0.096
Magnesium	1.02	0.330	0.019	0.136
Sodium	3.53	4.77	4.87	5.30
Bromide	0.0266	0.0313	0.011	0.0109
Chloride	5.86	5.36	4.8	5.24
Sulfate	0.177	0.216	0.170	0.182
Inorganic Carbon	Not reported	3.79×10^{-4}	0.016	4.55×10^{-4}
pH (standard units)	Not reported	8.82	6.17	8.99
pmH	Not reported	9.32	Not reported	9.93
Ionic Strength	7.44	6.44	5.32	5.99

All units are moles/L solution, unless otherwise specified.
Source: DOE (2014), except pmH values calculated using PHREEQC with ThermoChimie database

encapsulate and isolate the waste over geologic time scales. In addition, the Salado Formation is free of flowing water, easily mined, and geologically stable. While mostly free of water, hypersaline brines are present within Salado Formation fractures, inclusions, anhydrites, and clay seams. Hypersaline brines can also be present within fractures of the underlying Castile Formation. Repository excavation has disturbed the hydraulic gradient and resulted in brine seepage into the repository. In the absence of a drilling intrusion, it is expected that the volumes of brine in the repository will be relatively small and release of repository brine to the accessible environment is unlikely. However, WIPP is located in the Permian Basin, which hosts an abundance of oil and gas resources. Consequently, it is possible that future oil and gas drilling could inadvertently intrude into the repository and into underlying Castile brine, with subsequent direct removal of actinide-contaminated solid material and flow of repository brine to the surface. If repository brine reaches the ground surface, the concentrations of actinides dissolved in the brine will contribute to releases to the accessible environment.

WIPP waste consists of a variety of materials, including contaminated tools, clothing, soils, sludges, construction debris, rags, and other items left over from defense nuclear research and production. TRU waste eligible for WIPP disposal contains more than 100 nCi of alpha-emitting TRU isotopes per gram of waste with half-lives greater than 20 years, with high-level radioactive waste and selected other wastes excluded (U. S. Congress, 1996). Accepted waste includes radioactive elements with atomic numbers greater than 92, such as neptunium, plutonium, americium, and curium. Of these radionuclides, plutonium is expected to be one of the most important contributors to releases during the WIPP regulatory period. DOE currently estimates that 15 metric tons (MT) of plutonium will be placed in the repository (Van Soest, 2018), but is also considering disposing an additional 34 MT (NASEM, 2018).

Plutonium can exist in solution in the +III, +IV, +V and +VI oxidation states, and the plutonium oxidation state significantly affects its aqueous solubility and colloid formation (Choppin, 1991; Altmaier et al., 2013). Because electrolytically reducing conditions will prevail in deep geologic repositories such as WIPP, the most important long-term plutonium oxidation states will be +III and +IV (Altmaier and Geckeis, 2011). Pu(III) solids are generally more soluble than Pu(IV) solids (Kirsch et al., 2011; Felmy et al., 2012), so the oxidation state in the long-term WIPP repository will affect predicted plutonium solubilities in WIPP brines and the potential release of plutonium to the surface environment.

In this investigation, we evaluate the influence of repository processes and components on plutonium oxidation states by reviewing the scientific literature describing the effects of radiolysis, iron solids and aqueous species, organic ligands, humic substances, and microbial activity. We have supplemented this review with geochemical modeling, using recent aqueous speciation and solubility data to predict plutonium solubilities in brine under WIPP repository conditions. Results from both the review and the modeling calculations suggest that the Pu(III) oxidation state is likely to predominate in the aqueous and solid phases in the long-term WIPP repository environment. Our work also provides a blueprint for how other deep repositories could approach potential release scenarios over regulatory and geologic timescales by accounting for the interplay between actinide geochemistry, waste components, and rock mechanics. This investigation also highlights additional information necessary to create a more robust geochemical model for the prediction of plutonium solubility in high ionic strength systems.

2. Repository conditions

The WIPP repository is located in the Salado Formation, which is composed of halite interbedded by anhydrite layers. The Salado Formation halite layers also contain small quantities of anhydrite, gypsum [$CaSO_4{\cdot}2H_2O$(s)], polyhalite [$K_2MgCa_2(SO4)_4{\cdot}2H_2O$(s)], magnesite [$MgCO_3$(s)] and clays (DOE, 2014). The ambient temperature of the repository horizon is 28 °C and waste emplacement could increase temperatures by 3 °C (DOE, 2014). Underlying the Salado Formation is the Castile Formation, another evaporitic deposit composed of alternating carbonate, anhydrite, and halite beds.

Within the WIPP repository, large quantities of magnesium oxide [MgO(s)] are placed around the waste as an engineered barrier to control brine pH and carbonate concentrations (DOE, 2014). The MgO(s) hydrates upon brine or humid air contact, forming brucite [$Mg(OH)_2$(s)]. Brucite dissolution will buffer repository brine pmH at approximately 10–10.5.[1] Brucite will react with CO_2(g) to initially form hydromagnesite [$Mg_5(CO_3)_4(OH)_2{\cdot}4H_2O$(s)], which may eventually convert to magnesite [$MgCO_3$(s)]. Formation of hydromagnesite and magnesite is expected to maintain low CO_2(g) partial pressures (P_{CO2} $\sim 10^{-5.5}$ atm, Brush and Domski, 2013a) and low dissolved inorganic carbon concentrations (Table 1). Low dissolved inorganic carbon concentrations will minimize aqueous carbonate and bicarbonate complexation of actinides, and limit dissolved actinide concentrations in brine. WIPP waste will include an estimated 8884 MT of cement (Van Soest, 2018). This quantity of cement is not expected to significantly increase brine pmH values because mass balance calculations show that magnesium dissolved in brine and in polyhalite within the Salado Formation will be sufficient to buffer brine pmH through brucite precipitation (EPA, 2017).

[1] pmH equals the negative log of the molal hydrogen ion concentration.

After closure, brines will enter the repository either as seepage of intragranular and intergranular brine from the surrounding Salado Formation, or as a result of a drilling intrusion that passes through the repository into pressurized brine in the underlying Castile Formation (DOE, 2014). Seepage from the Salado Formation into the repository has been observed during operations and will continue after closure until hydrostatic equilibrium is re-established. Drilling through the repository into pressurized brine is less certain, is treated probabilistically in performance assessment (PA), and is modeled as occurring within the time period 100 years to 10,000 years post-closure (DOE, 2014). The compositions of these brines are represented by generic weep brine (GWB) for the Salado Formation and ERDA-6 brine for the Castile Formation (Table 1). The GWB brine composition is based on sampling of intergranular brines from the Salado Formation at or near the stratigraphic horizon of the repository (Snider, 2003). The ERDA-6 brine composition was obtained from brine samples from the ERDA-6 well near the WIPP repository, which is typical of pressurized brines from the Castile Formation (Popielak et al., 1983). After reaction with Salado Formation minerals and MgO(s) reaction products brucite and hydromagnesite, the repository brine composition ranges from the higher-magnesium composition of Salado brines to the lower-magnesium composition of Castile brines (Table 1).

The WIPP repository will contain an estimated 63,130 MT of iron-based metals and alloys at closure (Van Soest, 2018). Most will be emplaced as metallic iron [$Fe^0(s)$] in the steel waste containers, will be well-distributed throughout the repository, and in close contact with waste materials. The large amount of iron distributed throughout the repository will limit the development of oxic microenvironments. Initial oxic corrosion of these iron-based materials will consume the small amount of residual oxygen within a short period of time after the repository is sealed. After residual oxygen is consumed, iron corrosion will continue via anoxic corrosion reactions, producing $H_2(g)$. These reactions will occur when metallic iron reacts with brine, or with microbially produced $H_2S(g)$ or $CO_2(g)$ (DOE, 2014; Kim et al., 2017):

$$Fe^0(s) + (x+2)\ H_2O(l) \rightleftharpoons Fe(OH)_2{\bullet}xH_2O(s) + H_2(g) \quad (1)$$

$$3\ Fe^0(s) + 4\ H_2O(l) \rightleftharpoons Fe_3O_4(s) + 4\ H_2(g) \quad (2)$$

$$Fe^0(s) + H_2S(g) \rightleftharpoons FeS(s) + H_2(g) \quad (3)$$

$$Fe^0(s) + 2\ H^+ \rightleftharpoons Fe^{2+} + H_2(g) \quad (4)$$

$$Fe^0(s) + CO_2(g) + H_2O(l) \rightleftharpoons FeCO_3(s) + H_2(g) \quad (5)$$

Anoxic corrosion experiments conducted with WIPP brines have produced the Fe(II) solids ferrous hydroxide [$Fe(OH)_2{\bullet}xH_2O(s)$], FeS(s), and siderite [$FeCO_3(s)$] at the low temperatures anticipated in WIPP (Telander and Westerman, 1997). Magnetite [$Fe_3O_4(s)$], a mixed Fe(II)–Fe(III) oxide, may be thermodynamically stable under anticipated WIPP conditions and may also form over the long term due to anoxic iron corrosion (Selwyn, 2004; Saheb et al., 2010). Anoxic corrosion experiments in WIPP brines (Telander and Westerman, 1997) have not produced oxidized Fe(III) solids such as ferrihydrite [$Fe(OH)_3(s)$], and Fe(III) solids are expected to be unstable relative to more reduced phases such as $Fe(OH)_2{\bullet}xH_2O(s)$ and magnetite under repository redox conditions.

Hydrogen gas production through anoxic corrosion (reactions 1–5) will contribute to strongly reducing repository conditions. In addition to large amounts of metallic iron, other reductants will be present in the waste and waste containers, including metals such as aluminum and lead, organic ligands such as ethylenediaminetetraacetic acid (EDTA) in the waste, and humic substances in waste soils. Large amounts of sulfate will be available to repository brines because of the anhydrite interbeds in the Salado Formation (EPA, 2017). If microbial degradation of cellulosic, plastic or rubber (CPR) occurs, it should quickly consume the relatively small amounts of nitrate in the wastes, leaving sulfate in the brine as the most abundant electron acceptor available for microbial respiration (e.g., Lovley and Chapelle, 1995). Sulfate reduction will result in $H_2S(g)$ buildup and will outcompete methanogenesis, though small amounts of methane may still be produced in localized areas.

Table 2
Estimated WIPP plutonium inventory at closure (approximately 2033) and decayed to the end of the regulatory period (12,033).

Isotope	Half-Life (y)	Year 2033		Year 12,033	
		(grams)	(Ci)	(grams)	(Ci)
^{238}Pu	88	56,735	964,500	0.0	0.0
^{239}Pu	24,000	13,876,508	874,220	10,400,476	655,230
^{240}Pu	6500	1,387,652	319,160	483,174	111,130
^{241}Pu	14	18,653	1,865,300	0.1	12
^{242}Pu	380,000	40,975	164	41,250	165
Total	–	15,380,523	4,023,344	10,924,900	766,537

Source: Van Soest (2018).

Because large quantities of plutonium and other TRU elements will be placed in the repository (Table 2), alpha radiolysis may also affect repository conditions. Alpha radiolysis of CPR leads to the evolution of gases, including $H_2(g)$, carbon monoxide, $CO_2(g)$, and methane (O'Donnell, 1991). Relatively large quantities of CPR will be present in WIPP waste and packaging materials, including an estimated 4494 MT of cellulosics, 10,582 MT of plastics, and 1225 MT of rubber (Van Soest, 2018). Investigations of alpha radiolysis of CPR typical of WIPP waste demonstrated that radiolysis of these materials will predominantly generate $H_2(g)$ and $CO_2(g)$ (Molecke, 1980; Reed et al. 1992, 1998b; Reed and Molecke, 1993). Radiolysis will not cause increased P_{CO2} in WIPP because essentially all $CO_2(g)$ will react with the MgO(s) in the repository, but radiolysis of CPR will contribute to elevated post-closure repository $H_2(g)$ pressures.

Alpha irradiation of concentrated chloride solutions such as WIPP brines results in the production of gases [$H_2(g)$, $O_2(g)$ and $Cl_2(g)$] and oxidizing ionic species including hypochlorite [ClO^-], chlorite [ClO_2^-], and chlorate [ClO_3^-] (Kelm et al., 1999). Oxidizing radiolysis products are expected to react with the abundant iron in the repository and will not affect repository redox conditions (DOE, 2014). This expectation is based on the very high inventory of iron metals and alloys (63,130 MT) compared to the plutonium inventory (up to 49 MT) and the known rapid reactions between oxidizing ionic species such as chlorate and iron metal (e.g., Westerhoff, 2003). However, brine radiolysis will contribute to increased $H_2(g)$ pressures in the repository.

Cellulosic materials in cementitious environments can degrade to form isosaccharinic acid (ISA) (Van Loon and Glaus, 1997). Formation of ISA in repository brines could be important because ISA can form aqueous complexes with Pu(III) and Pu(IV) (Gaona et al., 2008; Tasi et al., 2018b). However, the pH range at which ISA production has been observed (approximately 12.5–13.4; e.g., Pavasars et al., 2003) significantly exceeds anticipated WIPP brine pmH values of 10–10.5. Pavasars et al. (2003) conducted cellulose degradation experiments at pH values that are comparable to expected WIPP conditions (8.4–10.2) and did not observe ISA production in this pH range. On this basis, significant formation of ISA in the WIPP repository is not anticipated.

Following repository closure, lithostatic and gas repository pressures may greatly increase from the initial 0.1 MPa (1 atm) because of volume reductions due to creep closure and Castile brine inflows (Fig. 1) and because of gas generation (Fig. 2). The gas phase within the sealed repository will include ambient air present at closure, gases generated by evaporation of volatiles in the waste, $H_2(g)$ produced by anoxic corrosion of iron metal, and $H_2(g)$ produced by radiolysis of brine and CPR in the waste and packaging materials. Microbial degradation of CPR may also produce $N_2(g)$ and $H_2S(g)$ in smaller amounts, as well as $CO_2(g)$. However, $CO_2(g)$ will be removed from the gas phase by reaction with the MgO(s) in the repository (DOE, 2014). Similarly, much of the $H_2S(g)$ will likely be removed through anoxic corrosion (reaction 3), while the relatively small amounts of produced $N_2(g)$ will remain unreactive. As a

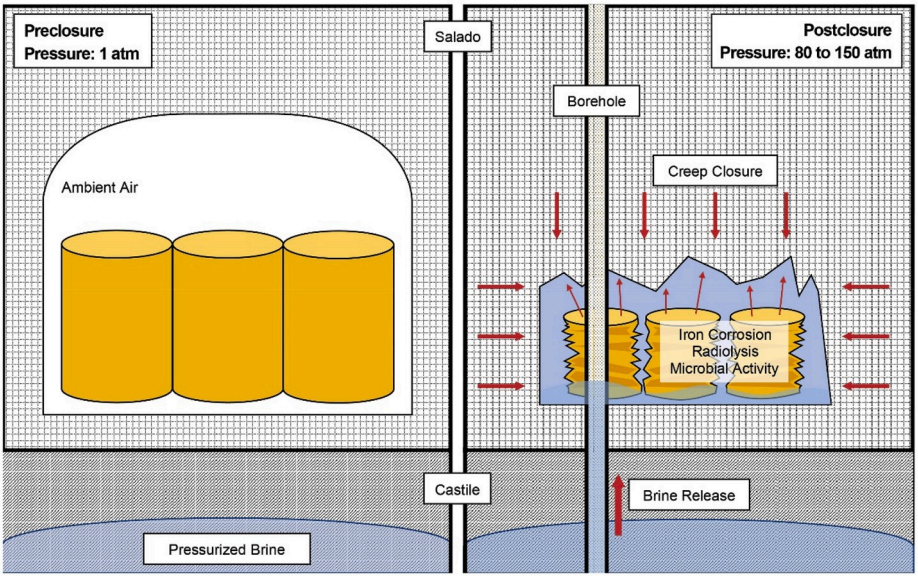


Fig. 1. Gas generation, drilling intrusion, and creep closure processes contributing to elevated pressures in the long-term WIPP repository.

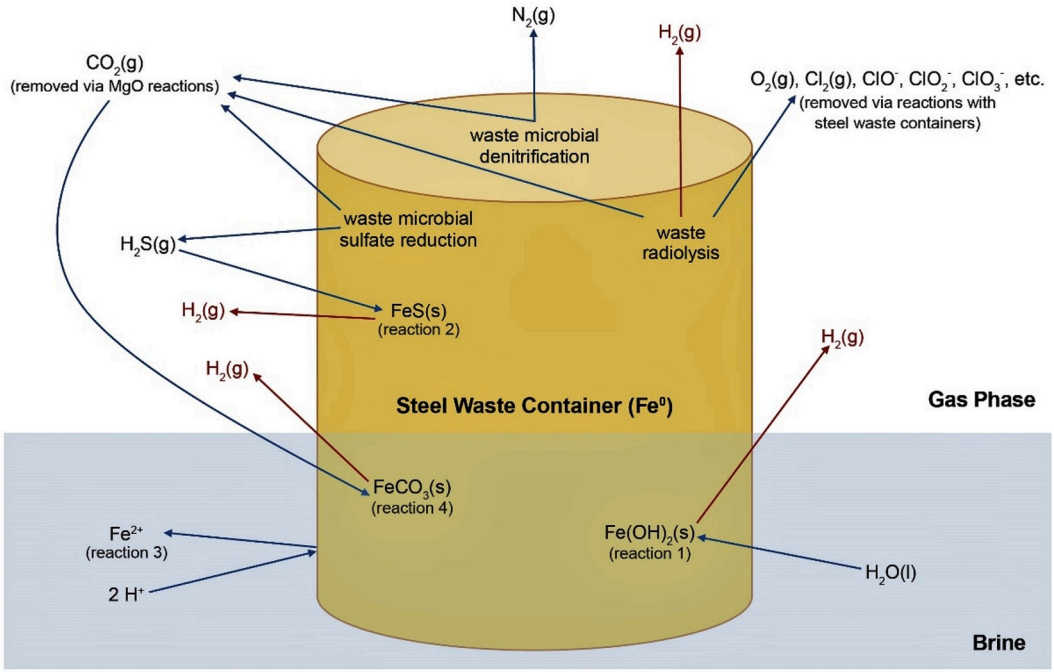


Fig. 2. Gas generation processes contributing to elevated pressures in the long-term WIPP repository.

result, $H_2(g)$ partial pressures [P_{H2}] from anoxic corrosion of iron-based metals and radiolysis of brines and CPR will account for much of the total gas pressure in the post-closure repository. The maximum post-closure pressure in the repository approximates the lithostatic pressure of 15 MPa (148 atm), because at higher pressures the anhydrite interbeds in the Salado are expected to fracture and allow gas to escape the repository (DOE, 2014). The minimum pressure for release of brine to the surface from the repository during a drilling intrusion is equal to the hydrostatic pressure of 8 MPa (79 atm), which is the pressure necessary for brine to flow from the repository to the surface (DOE, 2014). Because $H_2(g)$ will constitute the majority of the gas phase in the long-term repository, P_{H2} during release of brine to the surface would range from slightly less than 8 MPa to as high as 15 MPa.

The plutonium solid phases that will control repository brine solubilities are likely to be amorphous, hydrous Pu(III) and Pu(IV) solid phases:

$$Pu(OH)_3(am) + 3\ H^+ \rightleftharpoons Pu^{3+} + 3\ H_2O \quad (6)$$

$$PuO_2{\cdot}xH_2O(am) + 4\ H^+ \rightleftharpoons Pu^{4+} + (2 + x)\ H_2O \quad (7)$$

Because Pu(IV) solid phases are much less soluble than Pu(III) solid phases, the redox state of the plutonium solid can have significant effects on dissolved plutonium concentrations.

3. Solubility of Pu(III) and Pu(IV) solids

The available Pu(III) and Pu(IV) solubility and aqueous speciation data were evaluated for our prediction of possible dissolved plutonium

Table 3
Solubility constants for $Pu(OH)_3(s)$ and Pu^{3+} hydrolysis constants.

Reaction	log K_0 or β_n^0	Reference
$Pu(OH)_3(s) + 3\ H^+ \rightleftharpoons Pu^{3+} + 3\ H_2O$	15.8 ± 0.8	Felmy et al. (1989)
$Pu(OH)_3(s)$[a] $+ 3\ H^+ \rightleftharpoons Pu^{3+} + 3\ H_2O$ $Pu^{3+} + H_2O \rightleftharpoons PuOH^{2+} + H^+$	15.8 ± 1.5 -6.9 ± 0.3	NEA-TDB: Lemire et al. (2001), Guillaumont et al. (2003)
$Pu(OH)_3(am) + 3\ H^+ \rightleftharpoons Pu^{3+} + 3\ H_2O$ $Pu^{3+} + H_2O \rightleftharpoons PuOH^{2+} + H^+$	14.58 ± 0.5 -6.18 ± 0.25	Cho et al. (2016): from solubility and spectroscopic data
$Pu(OH)_3(s) + 3\ H^+ \rightleftharpoons Pu^{3+} + 3\ H_2O$ $Pu^{3+} + H_2O \rightleftharpoons PuOH^{2+} + H^+$	15.1 −6.9	Cho et al. (2016): Felmy et al. (1989) solubilitydata used with NEA-TDB log β_1^0 to recalculate log $K_{s,0}$
$Pu(OH)_3(s) + 3\ H^+ \rightleftharpoons Pu^{3+} + 3\ H_2O$ $Pu^{3+} + H_2O \rightleftharpoons PuOH^{2+} + H^+$	14.5 -6.18 ± 0.25	Cho et al. (2016): Felmy et al. (1989) solubility data used with Cho et al. (2016) log β_1^0 to recalculate log $K_{s,0}$
$Pu(OH)_3(s)$[a] $+ 3\ H^+ \rightleftharpoons Pu^{3+} + 3\ H_2O$ $Pu^{3+} + H_2O \rightleftharpoons PuOH^{2+} + H^+$ $Pu^{3+} + 2\ H_2O \rightleftharpoons Pu(OH)_2^+ + 2\ H^+$ $Pu^{3+} + 3\ H_2O \rightleftharpoons Pu(OH)_3^0 + 3\ H^+$	15.8 ± 1.5 -6.9 ± 0.3 −15.9 −25.3	ThermoChimie: solubility and first hydrolysis constant from NEA-TDB, second and third hydrolysis constants from Allard et al. (1980)
$Pu(OH)_3(s)$[a] $+ 3\ H^+ \rightleftharpoons Pu^{3+} + 3\ H_2O$ $Pu^{3+} + H_2O \rightleftharpoons PuOH^{2+} + H^+$ $Pu^{3+} + 2\ H_2O \rightleftharpoons Pu(OH)_2^+ + 2\ H^+$ $Pu^{3+} + 3\ H_2O \rightleftharpoons Pu(OH)_3^0 + 3\ H^+$	15.8 ± 1.5 -6.9 ± 0.3 -15.1 ± 0.7 -26.2 ± 0.5	Tasi et al. (2018a) solubility and first hydrolysis constant from NEA-TDB, second and third hydrolysis constants from Neck et al. (2007) by analogy with NEA-TDB hydrolysis constants for Am^{3+}

[a] – $Pu(OH)_3(s)$ designated as solid (s) because crystallinity was undetermined in Felmy et al. (1989) study, designated as crystalline (cr) in NEA-TDB compilations.

concentrations in WIPP brine that may be released to the surface during an inadvertent drilling intrusion.

3.1. Pu(III) solids

Few investigations have successfully measured the solubility of $Pu(OH)_3(am)$ because it is difficult to maintain adequately reducing experimental conditions. Felmy et al. (1989) conducted solubility experiments in an argon atmosphere using $^{239}Pu(III)$ stock solution. The experiments were conducted over a range of pH (6–13) for up to 24 days. The experiments were carried out in deionized water and in two chloride brines, PBB1 (I ~ 6 M) and PBB3 (I ~ 10 M). Higher solubilities were measured in the brines than in the deionized water. By analogy with Am^{3+}, the authors assumed that significant hydrolysis of the Pu^{3+} ion did not occur (Rai et al., 1983). Felmy et al. (1989) calculated a solubility constant (log $K_{s,0}$) using their low-ionic-strength solubility data (Table 3). It is likely that the Felmy et al. (1989) data represent the solubility of amorphous material because of the short duration of the experiments and the similar solubility results obtained by Cho et al. (2016) using amorphous $Pu(OH)_3(am)$, as discussed below. Because Felmy et al. (1989) did not directly evaluate the crystallinity of their solid phase, we have designated this phase as $Pu(OH)_3(s)$ to specify its undetermined crystallinity.

Lemire et al. (2001) reviewed and accepted the Felmy et al. (1989) log $K_{s,0}$ for the Nuclear Energy Agency Thermochemical Database Project (NEA-TDB) but increased its assigned uncertainty to ± 1.5 because of scatter in the solubility data and because of the steep slope of the solubility data vs. pcH[2] (Table 3). The solid phase in the NEA-TDB is designated as crystalline (Lemire et al., 2001; Guillaumont et al., 2003), but as previously noted, we refer to this material as $Pu(OH)_3(s)$, consistent with a phase that was likely amorphous but uncharacterized. Lemire et al. (2001) also evaluated the available Pu^{3+} hydrolysis data and derived a first hydrolysis constant (Table 3):

$$Pu^{3+} + H_2O \rightleftharpoons PuOH^{2+} + H^+ \quad (8)$$

[2] pcH equals the negative log of the molar hydrogen ion concentration.

The solubility constant and first hydrolysis constant from Lemire et al. (2001) are included in databases used for actinide geochemical modeling, including the ThermoChimie database (version 9b0, Giffaut et al., 2014). The second and third hydrolysis constants for Pu^{3+} in the ThermoChimie database (Table 3) were acquired from Allard et al. (1980), who obtained these values from Baes and Mesmer (1976).

Cho et al. (2016) investigated the solubility of $Pu(OH)_3(am)$ and the hydrolysis of Pu^{3+} by performing experiments with $^{242}Pu(III)$ in 0.1 M $NaClO_4$ at 25 °C and 0.1 MPa pressure. Coulometric titration was used to adjust the pH, with reducing conditions maintained electrolytically. The log β_1^0 for Pu^{3+} and log $K_{s,0}$ for $Pu(OH)_3(am)$ were evaluated using spectrophotometry to determine aqueous plutonium speciation, with laser-induced breakdown detection to identify colloid formation, and with x-ray diffraction to confirm that the plutonium solid remained amorphous during the experiments. Cho et al. (2016) used the Specific Ion Interaction Theory (SIT) data summarized by the NEA-TDB reviews (Lemire et al., 2001; Guillaumont et al., 2003) to extrapolate their experimental results to zero ionic strength (Table 3).

The Cho et al. (2016) solubility measurements are similar to the solubility measurements Felmy et al. (1989) obtained at low ionic strength. However, Cho et al. (2016) calculated a lower log $K_{s,0}$ because they determined that hydrolysis of Pu^{3+} was more important below pH 8–9 than Felmy et al. (1989) or the NEA-TDB had previously assumed (Table 3). The authors also found that calculations using the Felmy et al. (1989) solubility data and the NEA-TDB log β_1^0 resulted in a lower log $K_{s,0}$ than the NEA-TDB log $K_{s,0}$ value, whereas calculations using the Felmy et al. (1989) solubility data and the Cho et al. (2016) log β_1^0 resulted in a log $K_{s,0}$ that was essentially the same as the value calculated from the Cho et al. (2016) data (Table 3). The results of the Cho et al. (2016) investigation indicate that $Pu(OH)_3(am)$ is less soluble, and hence more stable, than indicated by the log $K_{s,0}$ calculated by Felmy et al. (1989). Cho et al. (2016) concluded that $Pu(OH)_3(am)$ is stable within the stability field of water at 1 atm.

3.2. Pu(IV) solids

Tasi et al. (2018a) investigated the solubility of nanocrystalline ^{242}Pu (IV) hydrous oxide [PuO_2(nc,hyd)] at 22 ± 2 °C in 0.1 M NaCl over a range of pH values under 0.1 MPa argon. Experiments were conducted

over a range of redox conditions maintained with no redox buffer, with hydroquinone buffer for mildly reducing conditions (pe + pmH = 9.5 ± 1), or with $SnCl_2$ buffer for more reducing conditions near the lower stability limit of water (pe + pmH = 2 ± 1). Aqueous plutonium concentrations in the hydroquinone-buffered experiments were extremely low (about $10^{-10.5}$ m) in the pmH range from 8 to 13 and were controlled by PuO_2(nc,hyd) in equilibrium with Pu(IV) aqueous species (reaction 7). The results of the unbuffered solubility experiments and hydroquinone-buffered solubility experiments yielded a log K_0 for PuO_2(nc,hyd) of −58.1 ± 0.3, in good agreement with the NEA-TDB value of −58.3 ± 0.5.

At the extremely low pe conditions of the $SnCl_2$-buffered experiments, aqueous plutonium concentrations were expected to be controlled by either the solubility of $Pu(OH)_3$(am) (reaction 6) or by the reductive dissolution of PuO_2(nc,hyd) to form aqueous Pu(III):

$$PuO_2(s) + 4\ H^+ + e^- \rightleftharpoons Pu^{3+} + 2\ H_2O \quad (9)$$

In $SnCl_2$-buffered experiments, x-ray absorption near-edge structure (XANES) spectra of the solids indicated an average Pu(III) content of 30 ± 5%. In addition, from about pH 8 to 9, solubility results were scattered and often exceeded the predicted solubility of PuO_2(nc,hyd). Tasi et al. (2018a) found these results were consistent with aqueous Pu(III) concentrations controlled by the solubility of either a mixture of PuO_2(nc, hyd) and $Pu(OH)_3$(am) or by a non-stoichiometric PuO_{2-x}(s) phase rather than simply reaction 9.

The ThermoChimie database includes solubility data for two amorphous, hydrous Pu(IV) solid phases with different reported solubilities (Table 4). As noted in the NEA-TDB reviews (Lemire et al., 2001; Guillaumont et al., 2003), "hydrous, amorphous" materials may not be unique and may vary in solubility depending upon factors such as aging of the material and radiolytic processes. The solubility constant for $Pu(OH)_4$(s) in the ThermoChimie database was determined from solubility experiments performed by Rai (1984), who used measured redox potentials and calculated activities of Pu^{4+}, PuO_2^+, and PuO_2^{2+} to account for multiple redox states of aqueous plutonium. The NEA-TDB solubility constant for $PuO_2{\cdot}2H_2O$(am) was derived using data from four more recent investigations (Capdevila and Vitorge, 1998; Knopp et al., 1999; Fujiwara et al., 2001; Rai et al., 2002).

Table 4
Solubility constants for hydrous, amorphous Pu(IV) solids and Pu^{4+} hydrolysis constants in the ThermoChimie database.

Reaction	log K_0 or β_n^0	Reference
$Pu(OH)_4$(am) + 4 H^+ ⇌ Pu^{4+} + 4 H_2O	−0.80 ± 1.3	Lemire and Garisto (1989), from Rai (1984)
$PuO_2{\cdot}2H_2O$(am) + 4 H^+ ⇌ Pu^{4+} + 4 H_2O	−2.37 ± 0.52	NEA-TDB: Guillaumont et al. (2003)
Pu^{4+} + H_2O ⇌ $PuOH^{3+}$ + H^+	0.60 ± 0.20	NEA-TDB: Guillaumont et al. (2003)
Pu^{4+} + 2 H_2O ⇌ $Pu(OH)_2^{2+}$ + 2 H^+	0.60 ± 0.30	NEA-TDB: Guillaumont et al. (2003)
Pu^{4+} + 3 H_2O ⇌ $Pu(OH)_3^+$ + 3 H^+	−2.30 ± 0.40	NEA-TDB: Guillaumont et al. (2003)
Pu^{4+} + 4 H_2O ⇌ $Pu(OH)_4^0$ + 4 H^+	−8.5 ± 0.50	NEA-TDB Guillaumont et al. (2003)

3.3. Plutonium stability at WIPP

The pe-pH[3] diagram of Fig. 3 illustrates our current understanding of the partitioning of 10^{-8} m plutonium in 3 m NaCl over a range of pe and pH values, based on calculations performed with the ThermoChimie database, using its solubility data for $Pu(OH)_4$(am) and $Pu(OH)_3$(s) (Giffaut et al., 2014). This figure was calculated at lower ionic strength than WIPP repository brines because the SIT approach for ionic strength correction is generally assumed to be reliable up to ionic strength of approximately 3.5 (e.g., Grenthe et al., 2013). Nonetheless, the figure approximates aqueous and solid-phase plutonium redox states and speciation at the higher ionic strengths of WIPP brines. Under the extremely reducing conditions near the lower stability limit of water, plutonium concentrations will be established by equilibrium between $Pu(OH)_3$(s) and Pu(III) dissolved aqueous species (reaction 6). Under less extreme reducing conditions, plutonium concentrations will be established by equilibrium between $Pu(OH)_4$(am) and dissolved Pu(IV) aqueous species (reaction 7). At intermediate redox conditions represented by the cross-hatched area in Fig. 3, $Pu(OH)_4$(am) will be in equilibrium with dissolved Pu(III) aqueous species (reaction 9), i.e., aqueous plutonium concentrations will be controlled by reductive dissolution. Fig. 3 shows that dissolved Pu(III) aqueous species and $Pu(OH)_3$(s) are stable under the reducing, alkaline pH conditions of WIPP repository brines. In contrast, Tasi et al. (2018a) calculated that Pu(III) solid would not be stable at 0.1 MPa and 0.1 m NaCl, using the lower solubility for $PuO_2{\cdot}2H_2O$(am) from the NEA-TDB. However, these calculations do not account for high P_{H2} in the WIPP repository, which extends the lower stability limit of water to lower pe/Eh values and makes the formation of $Pu(OH)_3$(s) and aqueous Pu(III) species more likely.

The experimental results obtained by Cho et al. (2016) at laboratory conditions of 0.1 MPa indicate that $Pu(OH)_3$(am) is more stable than the predicted values from ThermoChimie. Both the Cho et al. (2016) and Tasi et al. (2018a) studies indicate that significant Pu(III) solid may exist within the stability field of water at 0.1 MPa. These findings would extend the pe range at which Pu(III) solids are stable in Fig. 3 to higher values. Under the high P_{H2} conditions necessary for a release of brine to the surface from the WIPP repository (~8–15 MPa), the stability field of water extends to lower pe conditions and the formation of Pu(III) solids instead of Pu(IV) solids is even more likely.

4. Effects of WIPP repository conditions and processes on plutonium oxidation states

WIPP repository conditions and processes will affect aqueous and solid-phase plutonium oxidation states. Because of the large effects of plutonium aqueous and solid-phase oxidation states on predicted plutonium solubilities in WIPP brines, the expected plutonium oxidation states in the long-term WIPP repository can significantly affect predicted dissolved plutonium concentrations in brines released to the surface. There is uncertainty regarding the exact pe that will be established in the long-term WIPP repository under conditions where release of brine to the surface may occur. Consequently, the available information about conditions and processes that can affect plutonium oxidation states in the WIPP repository are reviewed below and the results of this review are used to establish reasonable limits on the redox conditions expected in the long-term WIPP repository.

4.1. Radiolysis

Upon repository closure, the WIPP waste inventory is currently predicted to include 15 MT of plutonium, which will decay to approximately 11 MT at the end of the WIPP repository performance period

[3] pe is defined as the negative logarithm of the electron activity.

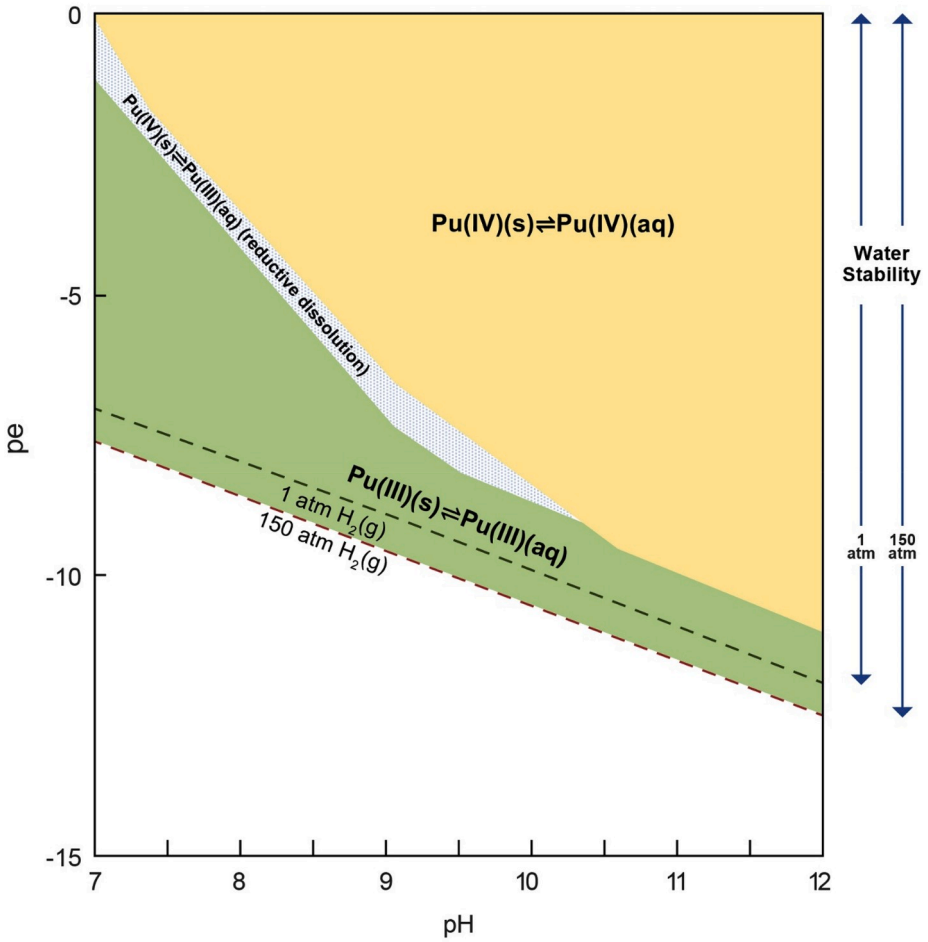


Fig. 3. Plutonium aqueous and solid-phase stabilities under alkaline, reducing conditions in 3 m NaCl, and 10^{-8} m total plutonium concentration.

(Table 2). However, an additional 34 MT of plutonium may be added to the inventory (NASEM, 2018). During the repository performance period, the largest percentage of plutonium by weight and by activity will be ^{239}Pu.

As discussed previously, the oxidizing effects of brine radiolysis on plutonium redox chemistry in the WIPP repository will likely be limited because the estimated 63,130 MT of iron-based metals and alloys emplaced throughout the repository will quickly react with radiolytically produced O_2(g) and oxidizing aqueous species (DOE, 2014; Westerhoff, 2003). On the other hand, radiolytically produced H_2(g) will persist and increase P_{H2} in the repository, potentially contributing to higher total gas pressures. In some reviewed plutonium solubility studies which included shorter-term experiments conducted with isotopes such as ^{239}Pu, solution radiolysis represents an experimental artifact that may have influenced results, creating the appearance that Pu(III) is far less stable than would be expected under anticipated repository conditions (e.g., the Ding et al., (2006) and Reed et al., (2006) studies discussed below). The half-life of ^{242}Pu (380,000 y) is much longer than the half-life of other plutonium isotopes (Table 2), so experiments conducted with ^{242}Pu would likely have smaller radiolytic effects.

4.2. Iron solids and aqueous species

Under anticipated conditions in the WIPP repository, multiple reduced iron solids and aqueous species could affect plutonium redox states including metallic iron, ferrous iron hydroxide solid, iron sulfide solids such as mackinawite [FeS(s)], siderite, magnetite, and aqueous ferrous iron. Reaction products of WIPP-specific iron corrosion experiments have identified only ferrous iron hydroxide reaction products and have indicated that ferric iron [Fe^{3+}] solids, such as ferrihydrite, will not form in the long-term WIPP environment (Telander and Westerman, 1997). Other investigations have identified magnetite as a potential reaction product of anoxic iron corrosion (Selwyn, 2004; Saheb et al., 2010).

A number of studies have evaluated the effects of iron solids and aqueous species on plutonium oxidation states in dilute solutions and in chloride brines (Supplementary Information, Table S1). Variables that likely influenced the results of these investigations include the iron solid or aqueous species, plutonium isotope and consequent radiolysis, solution composition, Pu(III) sorption on Fe surfaces, and duration of the experiments. Equilibration time is an especially important experimental variable because the regulatory timeframe for the WIPP is 10,000 years.

4.2.1. Investigations with metallic iron

Multiple short-term investigations (up to 11 weeks) conducted with metallic iron powder or iron coupons resulted in PuO_2(s) or $Pu(OH)_3$(s) and low aqueous plutonium concentrations of undetermined oxidation state (Xia et al., 2001 experiments in dilute NaCl, Ding et al., 2006; Reed et al., 2006). Radiolysis from ^{239}Pu may have influenced these results, leading to the formation of higher plutonium oxidation states, and the experiments may not have fully equilibrated during their relatively short durations. In a short-term experiment that was likely less affected by radiolysis because of the use of a longer-lived isotope, Reed et al. (2010) equilibrated ^{242}Pu for 2 weeks after adding metallic iron powder, iron coupons, or colloidal Fe(II) to WIPP brines. This experiment found that the iron solids reduced aqueous Pu(VI), resulting in Pu(IV) solid and low aqueous plutonium concentrations. Results from these short-term studies imply the stability of Pu(IV) solid and aqueous species in the

presence of metallic iron. However, these experiments may not have provided sufficient equilibration time.

Three longer-term (1.6–5.5 years) studies using plutonium and metallic iron allowed greater opportunity for equilibration and were carried out using ^{242}Pu in chloride brines to minimize radiolytic effects (Altmaier et al., 2009; Altmaier and Geckeis, 2011; Reed et al., 2011). Altmaier et al. (2009) investigated the solubility of ^{242}Pu(IV) hydrous oxide in 0.25 M and 3.5 M $MgCl_2$ solutions at approximately pcH 9 in the presence of metallic iron powder for periods up to 1.6 years. In these experiments, Pu(III) was the dominant oxidation state in solution. The solid phase was indirectly determined to be $PuO_2 \bullet xH_2O$(s) based on solubility calculations.

Altmaier and Geckeis (2011) investigated the plutonium solid phases, solubility, and aqueous speciation in 3.5 M $MgCl_2$ solutions under strongly reducing conditions with and without the presence of aqueous carbonate. Powdered metallic iron was used in the experiments to establish strongly reducing conditions, with ^{242}Pu used in the experiments conducted for up to 1.6 years. In experiments with Pu(IV) solid added to the solutions under carbonate-free conditions, plutonium solubilities were consistent with Pu(III) aqueous species in equilibrium with Pu(IV) solid (reaction 9). In a second set of carbonate-free experiments, addition of dissolved Pu(III) to the brine resulted in decreased plutonium concentrations over time again because of the formation of Pu(IV) solids in equilibrium with Pu(III) aqueous species (reaction 9). A third set of experiments was carried out by adding aqueous Pu(III) to brines containing precipitated Mg–OH–CO_3 solids to maintain low carbonate concentrations. In these experiments, Pu(III) solid was in equilibrium with Pu(III) aqueous species over the entire 1.6-year experimental duration (reaction 6), likely because carbonate strongly complexed and stabilized Pu(III) in the solid phase.

Reed et al. (2011) reported the results of ^{242}Pu(VI)-brine experiments with added iron coupons or iron powder that were equilibrated for about 5.5 years. Analysis of the plutonium solid phase indicated that it was 90%–100% Pu(III). Transformation over time of the initially formed Pu(IV) solids to Pu(III) solids coincided with an increase in aqueous plutonium concentrations, consistent with higher $Pu(OH)_3$(am) solubility (reaction 6).

The longer-term experimental results with ^{242}Pu and iron metal in brines (Altmaier et al., 2009; Altmaier and Geckeis, 2011; Reed et al., 2011) indicate that at atmospheric pressures, aqueous plutonium is likely to be in the Pu(III) oxidation state under strongly reducing conditions established by interaction of iron metal with brines. Both Pu(III) and Pu(IV) solids formed in these experiments, consistent with the control of plutonium solubilities by reactions 6 and 9, respectively. In the longest-term (5.5 year) experiments (Reed et al., 2011), predominantly Pu(III) solid formed (reaction 6), with Pu(III) present in the aqueous phase.

4.2.2. Experiments with Fe^{2+} and iron oxides

Other investigations (Rai et al., 2002, Felmy et al., 2011, 2012) have demonstrated that aqueous Fe^{2+} in dilute chloride solutions and brines leads to reductive dissolution of PuO_2(s) to form aqueous Pu(III) species (reaction 9). Reed et al. (2006) found that Fe^{2+} reduced Pu(VI) dissolved in WIPP brines and resulted in precipitation of Pu(IV) solid containing possible minor amounts of Pu(III) solid at pcH 7 to 10.

Additional experiments investigated plutonium interactions with magnetite (Reed et al., 2010, Kirsch et al., 2010, 2011). Reed et al. (2010) reported the results of short-term experiments to evaluate the effects of magnetite on ^{242}Pu(VI) reduction in ERDA-6 brine. The experiments were carried out in brine containing carbonate ion at pcH 9. XANES analysis showed that aqueous Pu(VI) was reduced to form a solid Pu(IV) phase, and magnetite also quickly reduced plutonium concentrations in solution. Reed et al. (2011) reported additional, longer-term results (5.5 years) for experiments that evaluated the interaction of ^{242}Pu(VI) in brine with magnetite at approximately pH 9. PuO_2(s) was the initial solid phase formed in these experiments, which transformed over time to 87% Pu(III) solid. Transformation from Pu(IV) to Pu(III) solids coincided with an increase in aqueous plutonium concentrations, consistent with higher $Pu(OH)_3$(am) solubility.

Kirsch et al. (2010, 2011) carried out a series of experiments in 0.1 M NaCl, contacting solutions of ^{242}Pu(III) with magnetite at pH values of approximately 6 and 8, or contacting solutions of ^{242}Pu(V) with magnetite or mackinawite at pH values of approximately 8. After approximately 40 days, aqueous plutonium concentrations were below the analytical detection limit of 1×10^{-9} M. Pu(III) and Pu(V) added to magnetite was immobilized on the magnetite surface as a Pu(III) surface complex. The Pu(V) added to mackinawite was immobilized as PuO_2(s). This reduction to Pu(IV) solid instead of Pu(III) solid by mackinawite may have been related to the relatively short time period of weeks instead of years for the experiments.

Longer-term experiments investigating the reaction of magnetite with Pu(VI) indicate that significant Pu(III) solid formation will occur over the long time periods applicable to WIPP (Reed et al., 2011). Relatively short-term experiments (Rai et al., 2002, Reed et al., 2006, Felmy et al., 2011, 2012) indicate that Fe^{2+} leads to reductive dissolution of Pu(IV) solid (reaction 9), and other short-term experiments (Kirsch et al., 2010, 2011) show that magnetite sorbs aqueous Pu(III) and mackinawite reduces aqueous Pu(V) to Pu(IV) solid.

4.2.3. Effects of iron under WIPP conditions

The studies that are most applicable to the long-term WIPP repository environment are Reed et al. (2011), Altmaier et al. (2009), and Altmaier and Geckeis (2011). These experiments demonstrated that metallic iron and magnetite cause Pu(III) to be present in solution. In the solid phase, either Pu(III) or Pu(IV) solids were observed or inferred over the short term, but Pu(III) solids formed in long term experiments in WIPP brines with metallic iron or magnetite (Reed et al., 2011). Investigations of the effects of aqueous ferrous iron on plutonium redox state in the presence of goethite and magnetite indicate that PuO_2(am) undergoes reductive dissolution to aqueous Pu(III) (Felmy et al., 2011, 2012). The available data in these studies indicate that metallic iron, iron sulfides, magnetite, and aqueous ferrous iron in WIPP repository brines are likely to result in the formation of Pu(III) and Pu(IV) solids in equilibrium with aqueous Pu(III). These experiments, which were conducted at atmospheric pressures, do not account for strongly reducing conditions and the long time periods relevant to the sealed long-term WIPP repository. The highly reducing conditions brought about by the presence of metallic iron, ferrous hydroxide solids and magnetite as well as the long equilibration period will stabilize more reduced [Pu(III)] aqueous species and solid phases.

4.3. Organic ligands and humic substances

WIPP waste will contain organic ligands including EDTA, oxalate, citrate, and acetate (Table 5). As discussed previously, significant ISA formation is not expected in WIPP because of the expected mildly alkaline pH ranges of the repository brine (e.g., Pavasars et al., 2003). Although organic ligands may be consumed by microbes, the highly saline environment may limit microbial activity (NEA, 2018) and organic ligands may persist for some time in the repository. Additionally, humic substances are likely to be present in waste soils placed in the repository. The organic ligands and humic substances may form stable

Table 5
Predicted organic ligand concentrations in WIPP inventory and brines (Brush and Domski, 2013b).

Organic Ligand	Inventory (kg)	Brine Concentration (M)
Acetate (as acetic acid)	24,100	$4.61 \times 10^{-3} - 2.30 \times 10^{-2}$
Citrate (as citric acid)	7880	$4.65 \times 10^{-4} - 2.33 \times 10^{-3}$
EDTA	376	$1.48 \times 10^{-5} - 7.40 \times 10^{-5}$
Oxalate (as oxalic acid)	18,400	$2.36 \times 10^{-3} - 1.18 \times 10^{-2}$

complexes with aqueous plutonium and influence plutonium oxidation states in WIPP brines.

Studies have established that organic ligands are capable of reducing Pu(V) and Pu(VI) species under WIPP-relevant conditions (Reed et al., 1996, 1998). Other studies show that EDTA may affect the redox states of Pu(III) and Pu(IV) (AlMahamid et al., 1996; Boukhalfa et al., 2003; Boukhalfa et al., 2004; Rai et al., 2008). Of these investigations, the Rai et al. (2008) experiments that included iron are the most relevant to WIPP repository conditions and these results indicate that in the presence of aqueous ferrous iron and EDTA, Pu(IV) solids can undergo reductive dissolution to aqueous Pu(III). Considering the anticipated concentration of EDTA and organic ligands relative to plutonium in the repository, as well as the availability of reduced aqueous iron species, the experiments performed by AlMahamid et al. (1996) and Rai et al. (2008) show that EDTA may stabilize Pu(III), enhance the reductive dissolution of Pu(IV), and increase Pu(III) mobility in WIPP brine.

Humic and fulvic acids present in WIPP waste are also potentially important for plutonium reduction (Choppin, 1991; André and Choppin, 2000; Marquardt et al., 2004; Marquardt et al., 2008; Banik, 2006). Collectively, these studies indicate that Pu(V) and Pu(VI) likely will be reduced by humic substances to a mixture of Pu(III) and Pu(IV).

Overall, investigations of the effects of organic ligands and humic substances on plutonium oxidation states indicate that these substances tend to reduce Pu(V) and Pu(VI) to Pu(III) and Pu(IV). In the presence of small amounts of ferrous iron, EDTA promotes the reductive dissolution of Pu(IV) solids, and Pu(III)-EDTA complexes appear likely to form, stabilizing the aqueous Pu(III) oxidation state.

4.4. Microorganisms

Microorganisms have been identified in WIPP halite (Swanson, 2013) and actively metabolizing microorganisms may also be introduced into the repository with the waste or by the ventilation system from the outside environment. However, the highly saline environment and potential toxicity created by actinides in WIPP may limit microbial activity (NEA, 2018). Active microorganisms may cause either direct or indirect reduction of plutonium. Evidence obtained in low-ionic-strength experiments shows microbial plutonium reduction could occur (Rusin et al., 1994; Bolton et al., 2006; Boukhalfa et al., 2007; Francis et al., 2007; Icopini et al., 2009; Renshaw et al., 2009; Plymale et al., 2012).

More limited data relevant to microbial reduction of plutonium are available for high-ionic-strength solutions such as WIPP repository brines. Reed et al. (2011) observed reduction of Fe(III) to Fe(II) by a mixed culture of halophilic Bacteria and Archaea at 2.5–3.5 M ionic strength. Production of aqueous ferrous iron could cause subsequent reduction of Pu(IV) to Pu(III). Emmerich et al. (2012) performed experiments with mixed cultures from a hypersaline lake demonstrating that microbial reduction of Fe(III) can occur in brines with NaCl concentrations up to 5 M. Because of the limited high-ionic-strength data, microbial reduction of plutonium in WIPP brines is highly uncertain.

5. Modeling plutonium solubilities in WIPP brines

Review of the available scientific literature has shown that under reducing conditions at atmospheric pressure, plutonium is likely to be present as Pu(III) aqueous species in equilibrium with Pu(III) or Pu(IV) solid phases (reactions 6 and 9, respectively). Strongly reducing WIPP conditions are facilitated by iron in the waste and waste containers and possibly organic ligands and microorganisms. WIPP repository pressures may reach 8–15 MPa, which are the pressures necessary to release brine to the ground surface following a borehole intrusion (DOE, 2014). A significant fraction of the repository gas phase will consist of H_2(g), which will establish extremely reducing conditions in the repository, increasing the pe ranges at which water is stable as well as the range at which Pu(III) solids and aqueous species will exist (Fig. 3). We used the following geochemical modeling calculations to further evaluate the effects of highly reducing conditions at elevated total pressures on plutonium oxidation states in WIPP brines.

5.1. Model assumptions and inputs

The WIPP PA includes calculations of actinide solubilities in WIPP brines using EQ3/6 geochemical modeling code (Wolery et al., 2010) and a project-specific thermodynamic database that includes Pitzer parameters to correct for high ionic strength. Use of the Pitzer approach for ionic strength correction is generally accepted for aqueous solutions with an ionic strength greater than approximately 3.5. However, because Pitzer data are experimentally derived, much of the information in the WIPP database is incomplete and the database does not include redox reactions for plutonium or iron aqueous and solid phases. We therefore opted to use the ThermoChimie database (version 9b0, Giffaut et al., 2014) and the PHREEQC geochemical modeling code (version 3.3.8, Parkhurst and Appelo, 2013) to perform solubility and aqueous speciation calculations. ThermoChimie is a publicly available, internally consistent database that includes relevant plutonium and iron aqueous species and solid phases, mostly based on the NEA-TDB data, but with some additional solids and aqueous species. The ThermoChimie database uses the SIT approach to correct for ionic strength effects. The SIT approach is reliable up to ionic strengths of approximately 3.5, although for some constituents in different ionic media, it can be accurate up to ionic strengths of 6–10 (Giffaut et al., 2014). All calculations were performed at 25 °C and 150 atm total pressure, over a range of P_{H2}.

Laboratory testing in WIPP brines has demonstrated that repository iron, including metallic iron-containing waste and container steel, will corrode to form Fe(II) solids, such as $Fe(OH)_2$(cr) or siderite and that more oxidized Fe(III) solids such as ferrihydrite will not be stable (Telander and Westerman, 1997; Kim et al., 2017). Other investigations have established that magnetite may also form during anoxic iron corrosion (e.g., Smart et al., 2001; Saheb et al., 2010). Consequently, the conditions where $Fe(OH)_2$(cr) is in equilibrium with magnetite establishes a reasonable upper limit for pe in the repository. An alternative upper pe limit for the WIPP repository under conditions where a brine release could occur is the pe corresponding to a P_{H2} of approximately 8 MPa. This alternative upper limit was not used because there is uncertainty regarding whether plutonium oxidation states would be in equilibrium with the hydrogen gas pressure, whereas experimental data have indicated that plutonium oxidation states react with iron metal and magnetite in a reasonably short time period (~5.5 years, Reed et al., 2011) compared to the time period when brine release to the surface may occur (100–10,000 years). The lower limit of the pe in the WIPP repository is established by the maximum P_{H2} of approximately 15 MPa in equilibrium with $Fe(OH)_2$(cr).

Because the SIT approach is optimized for lower ionic strength solutions than WIPP brines, plutonium solubilities and aqueous speciation were calculated for 0.1 m NaCl and for diluted (1:4) GWB and ERDA-6 WIPP brines to understand general plutonium oxidation state trends. While acknowledging the uncertainties related to modeling high ionic strength using SIT, we also modeled full-strength GWB and ERDA-6 brines to infer how modeled plutonium solubilities and aqueous speciation at low ionic strength compare at high ionic strength. For each set of calculations, brine was first equilibrated with the Salado Formation mineral anhydrite, to represent brine contact with repository minerals, as well as the minerals brucite and hydromagnesite formed by MgO(s) hydration and carbonation to establish pH and P_{CO2} conditions. For the full-strength WIPP brine calculations, the brine was also initially equilibrated with halite. The equilibrated brines were then used in a series of calculations at constant pH and P_{CO2} with addition of 0.001 m $PuO_2{\cdot}2H_2O$(am) and 0.1 m $Fe(OH)_2$(cr) over a range of pe values established by varying P_{H2} from 1×10^{-8} MPa–15 MPa. In these calculations, using $PuO_2{\cdot}2H_2O$(am) as the hydrous, amorphous Pu(IV) solid increased the calculated stability field for Pu(IV) solid in the resulting

figures relative to the results obtained using the higher solubility for Pu $(OH)_4$(am) (not shown). $PuO_2{\cdot}2H_2O$(am) was included as the stable Pu (IV) solid phase instead of $Pu(OH)_4$(am) to maximize the pe range over which the Pu(IV) solid phase is more stable than the Pu(III) solid phase. To evaluate the potential effects on dissolved plutonium concentrations of the organic ligands identified in WIPP waste (acetate, citrate EDTA, and oxalate), additional modeling calculations were performed. These calculations would be expected to overestimate the effects of organic ligands because of possible microbial consumption of these organic compounds.

WIPP brines contain borate species ranging from 0.06 M to 0.16 M total boron (Table 1) and there is evidence that borate can influence Pu (III) aqueous speciation and solubilities. Schott et al. (2014) and Hinz et al. (2015) using Eu(III) and Nd(III) analogues, respectively, determined that precipitation of +III actinides as borate solids could significantly reduce +III actinide solution concentrations in circumneutral to mildly alkaline (pcH up to 9) solutions. On the other hand, Borkowski et al. (2010) determined that total boron concentrations up to 0.16 M increased Nd(III) concentrations in NaCl solutions up to 5 M. The results of these studies indicate that borate and polyborate species in WIPP brines could affect Pu(III) solubilities. Because of the differences between the results of Borkowski et al. (2010) and those of Schott et al. (2014) and Hinz et al. (2015) and because the ThermoChimie database does not include Pu(III)-borate aqueous species or solid phases, the modeling calculations do not include the potential effects of borate on Pu(III) solid solubilities. The possible effects of borate aqueous complexation with Pu(III) and precipitation of a Pu(III)-borate solid phase on aqueous Pu(III) concentrations add to the uncertainty associated with the calculated Pu(III) solid solubilities.

5.2. Model results and discussion

Model-calculated plutonium solubilities at 0.1 m NaCl and pe ~ −7.1 fall within the range of $SnCl_2$-buffered experimental results from Tasi et al. (2018a) at pmH 9.0 (Fig. 4), providing verification that our models adequately simulate the existing data. The Tasi et al. (2018a) experiments were conducted at redox conditions more oxidizing than predicted for the long-term WIPP repository (Fig. 4). In the 0.1 m NaCl solution, the ThermoChimie calculations predict $PuO_2{\cdot}2H_2O$(am) as the solubility-controlling phase with both Pu(III) and Pu(IV) aqueous species contributing to total dissolved plutonium concentrations at the pe conditions of the Tasi et al. (2018a) experiments. At this pe and pmH, Tasi et al. (2018a) determined that the solid phase was composed of up to 30% Pu(III), as either a mixture with Pu(IV) solid or as a PuO_{2-x} solid phase, a phase that currently cannot be modeled using existing datasets.

Under conditions in 0.1 m NaCl where pe is equal to or more reducing than the equilibrium between $Fe(OH)_2$(cr) and magnetite (pe ≤ -10), the modeling results indicate that Pu(III) aqueous species will be in equilibrium with $Pu(OH)_3$(s) (reaction 6). It is also notable that Pu (III) will predominate as the major solid phase and aqueous plutonium species even at pe ranges more oxidizing than expected WIPP conditions (Fig. 4).

Figs. 5 and 6 illustrate the results from the modeling calculations in more complex solutions using 1:4 diluted ERDA-6 brine (I = 2.5) and undiluted ERDA-6 brine (I = 7.7 to 7.8), respectively. Modeling calculations with 1:4 diluted GWB and undiluted GWB produced comparable results (Figs. 7 and 8) to those obtained using ERDA-6 brine. The P_{CO2} was calculated to be $10^{-5.8}$ atm for all four diluted and full-strength brines.

In diluted WIPP brines (Figs. 5 and 7), Pu(III) and Pu(IV) aqueous and solid phase stabilities followed similar patterns as in 0.1 m NaCl (Fig. 4), with Pu(III) solids and aqueous species controlling plutonium solubilities under condition more reducing than the equilibrium between $Fe(OH)_2$(cr) and magnetite. The results additionally demonstrate that Pu(III) solids and aqueous species are stable over a wide pe range that extends to pe values higher than expected repository conditions. Our calculated plutonium solubilities under WIPP redox conditions are approximately two orders of magnitude greater in full-strength brines (Figs. 6 and 8) than dilute brines (Figs. 5 and 7), showing that plutonium solubilities will increase with increasing ionic strength, consistent with the results obtained by Felmy et al. (1989) in deionized water and different high-ionic-strength brines. Furthermore, WIPP-relevant H_2(g) pressures are shifted to lower pe values in full-strength brines compared to low-ionic-strength brines. This indicates that the effect of high ionic strength on P_{H2} will be to decrease pe, further increasing the ranges at which Pu(III) is stable (Fig. 3).

Modeled aqueous Pu(III) concentrations in equilibrium with Pu $(OH)_3$(s) ranged from 3×10^{-7} m in pmH 9.16 GWB to 2×10^{-6} m in pmH 9.93 ERDA-6 brine. There is considerable uncertainty associated with these modeled concentrations because: 1) the ionic strengths of the brines exceed the ionic strength generally accepted for using the SIT approach, 2) the ThermoChimie database does not include solubility data for potential Pu(III)-borate solids that may precipitate in the WIPP repository (Schott et al., 2014; Hinz et al., 2015) or stability constants

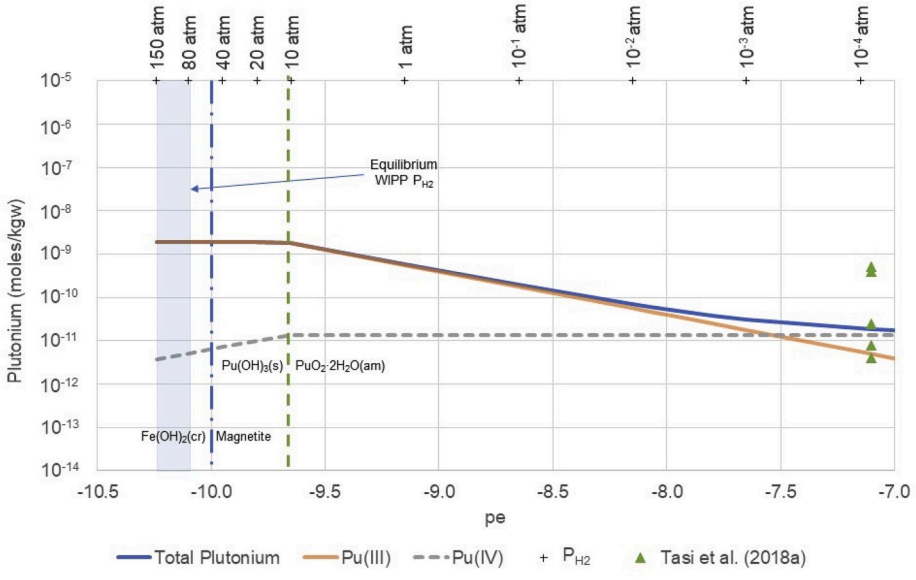


Fig. 4. Total, Pu(III), and Pu(IV) aqueous concentrations calculated as a function of pe in 0.1 m NaCl at pmH 9.05. Solubility results of Tasi et al. (2018a) obtained in $SnCl_2$-buffered solutions are also presented. WIPP equilibrium redox conditions (vertical blue shaded area) consistent with brine release are constrained by the equilibrium of $Fe(OH)_2$(cr) with H_2(g) at P_{H2} from 80 to 150 atm. The equilibrium between $Fe(OH)_2$(cr) and magnetite, representing the upper limit of pe in the repository, is indicated by the dashed vertical blue line. The dashed green vertical line indicates the pe at which $Pu(OH)_3$(s) is in equilibrium with $PuO_2{\cdot}2H_2O$(am).

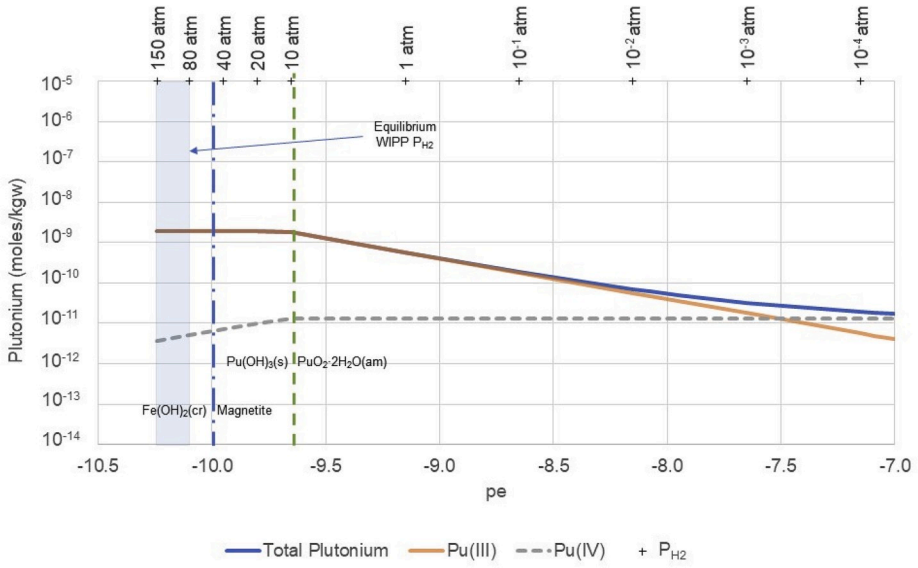


Fig. 5. Total, Pu(III), and Pu(IV) aqueous concentrations calculated as a function of pe in diluted ERDA-6 brine at pmH 9.25 and $P_{CO2} = 10^{-5.8}$. WIPP equilibrium redox conditions (vertical blue shaded area) are constrained by the equilibrium of $Fe(OH)_2$(cr) with H_2(g) from approximately 80 to 150 atm P_{H2}. The equilibrium between $Fe(OH)_2$(cr) and magnetite, representing the upper limit of pe in the repository, is indicated by the dashed vertical blue line. The dashed green vertical line indicates the pe at which $Pu(OH)_3$(s) is in equilibrium with $PuO_2{\cdot}2H_2O$(am).

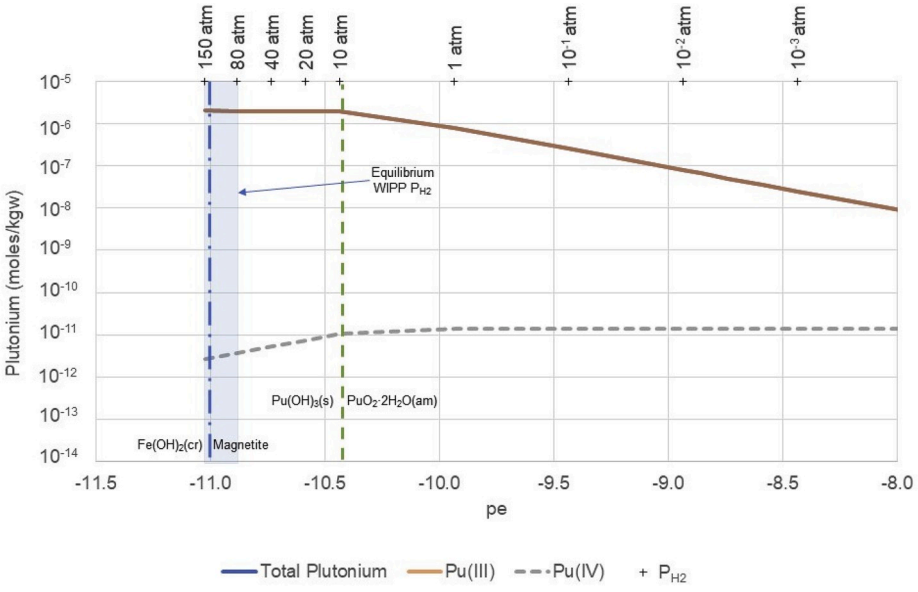


Fig. 6. Total, Pu(III), and Pu(IV) aqueous concentrations calculated as a function of pe in full-strength ERDA-6 brine at pmH 9.93 and $P_{CO2} = 10^{-5.8}$. WIPP equilibrium redox conditions (vertical blue shaded area) are constrained by the equilibrium of $Fe(OH)_2$(cr) with H_2(g) from approximately 80 to 150 atm P_{H2}. The equilibrium between $Fe(OH)_2$(cr) and magnetite, representing the upper limit of pe in the repository, is indicated by the dashed vertical blue line. The dashed green vertical line indicates the pe at which $Pu(OH)_3$(s) is in equilibrium with $PuO_2{\cdot}2H_2O$(am). Note that the x axis in this figure is offset by 1 pe unit relative to Figs. 4, 5, 7 and 8.

for potential Pu(III)-borate aqueous species (Borkowski et al., 2010), and 3) recent $Pu(OH)_3$(am) solubility data Cho et al., (2016) indicate that Pu(III) solids may be less soluble than modeled using the solubility constant from Felmy et al. (1989) that is included in ThermoChimie.

Though using SIT to correct for ionic strength introduces uncertainty to the model results at high ionic strength, we can infer that the most significant effect of increased ionic strength between dilute solutions and WIPP brines will be higher dissolved plutonium concentrations. Using the ThermoChimie database to simulate the solubility results of Felmy et al. (1989) in high-ionic-strength brines resulted in fair agreement between the measured solubilities and modeling calculations at slightly alkaline pcH values of about 7.5–8.5, but more significant differences under more alkaline conditions (Supplementary Information, Figs. S1 and S2).

For all of the solubility calculations including 0.1 m NaCl, diluted WIPP brines, and undiluted WIPP brines, corresponding model-calculated oxygen fugacities [f_{O2}] ranged from 10^{-91} at P_{H2} equal to 15 MPa to 10^{-86} at P_{H2} equal to 0.1 MPa. This range is slightly more oxidizing than the f_{O2} value of $10^{-91.2}$ calculated for the WIPP repository based on the equilibrium between metallic iron and siderite at pH 8.9 and a bicarbonate [HCO_3^-] concentration of $10^{-3.3}$ (Kim et al., 2017), and is slightly more reducing than the f_{O2} of 10^{-85} calculated for the equilibrium between metallic iron and Fe-hibbingite [$Fe_2(OH)_3Cl$(s)] at pH 9 (Nemer et al., 2011). These results show that the redox conditions modeled in this investigation are reasonably consistent with the conditions predicted for the WIPP repository in other investigations.

We performed additional calculations using the full-strength ERDA-6 brine and the maximum predicted concentrations of the organic ligands acetate, citrate, EDTA, and oxalate (not shown). These potential complexing agents did not affect the plutonium solubility results due to fairly low organic ligand concentrations and the presence of iron, calcium, and magnesium ions in the brine which preferentially complexed with the organic ligands.

Our modeling results in WIPP brines include uncertainties stemming from extending the SIT model to ionic strengths greater than 3.5, and development of a comprehensive Pitzer-based database that is optimized for high ionic strengths would decrease these uncertainties. Additional uncertainty is associated with our modeling results because

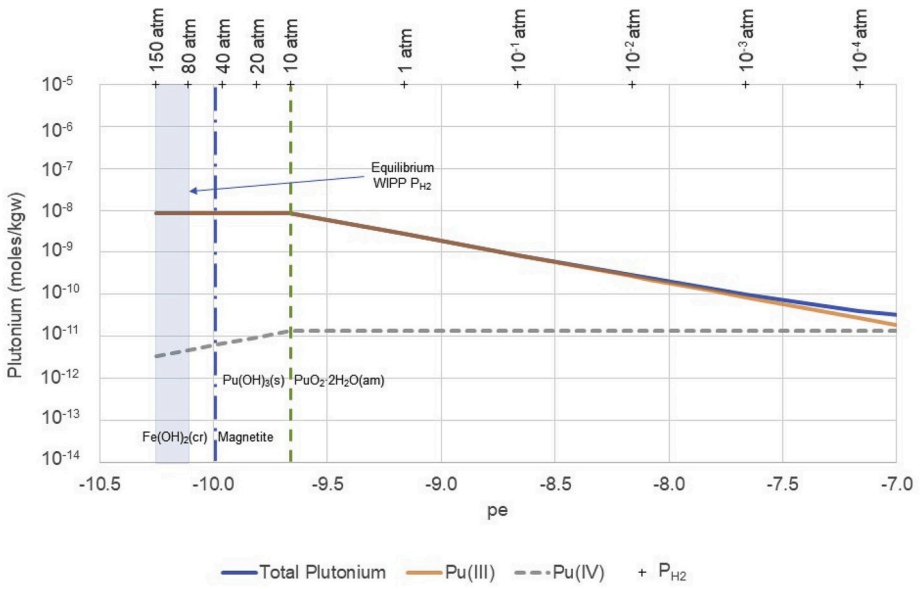


Fig. 7. Total, Pu(III), and Pu(IV) aqueous concentrations calculated as a function of pe in diluted GWB at pmH 9.16 and $P_{CO2} = 10^{-5.8}$. WIPP equilibrium redox conditions (vertical blue shaded area) are constrained by the equilibrium of $Fe(OH)_2$(cr) with H_2(g) from approximately 80 to 150 atm P_{H2}. The equilibrium between $Fe(OH)_2$(cr) and magnetite, representing the upper limit of pe in the repository, is indicated by the dashed vertical blue line. The dashed green vertical line indicates the pe at which $Pu(OH)_3$(s) is in equilibrium with $PuO_2{\cdot}2H_2O$(am).

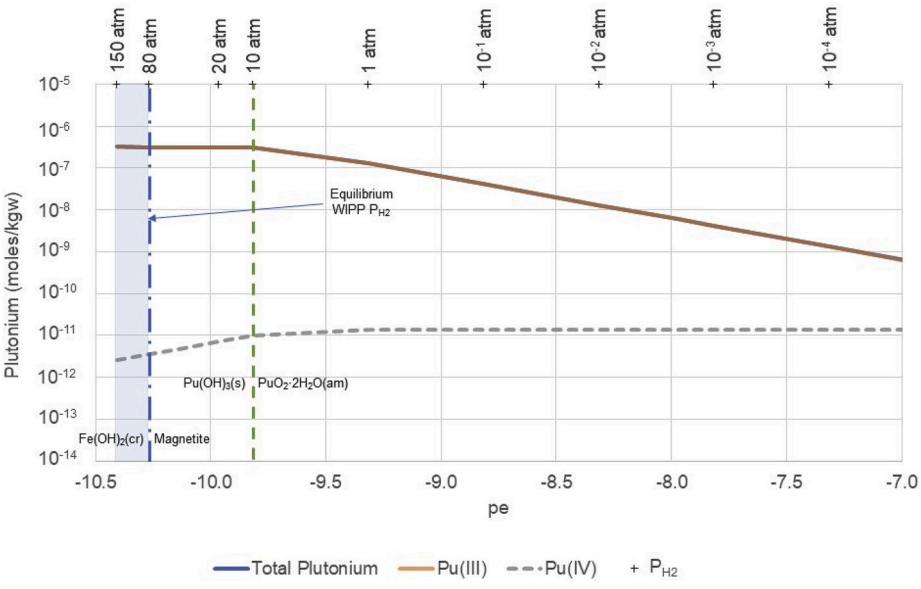


Fig. 8. Total, Pu(III), and Pu(IV) aqueous concentrations calculated as a function of pe in undiluted GWB at pmH 9.32 and $P_{CO2} = 10^{-5.8}$. WIPP equilibrium redox conditions (vertical blue shaded area) are constrained by the equilibrium of $Fe(OH)_2$(cr) with H_2(g) from approximately 80 to 150 atm P_{H2}. The equilibrium between $Fe(OH)_2$(cr) and magnetite, representing the upper limit of pe in the repository, is indicated by the dashed vertical blue line. The dashed green vertical line indicates the pe at which $Pu(OH)_3$(s) is in equilibrium with $PuO_2{\cdot}2H_2O$(am).

of varied data regarding the nature of the Pu(III) solid that forms at extremely low pe values (Cho et al., 2016; Tasi et al., 2018a), which highlights the need for additional experimental data under these conditions. Despite the uncertainties we have identified, our SIT model-based calculations provide a useful qualitative indication of the effects of high ionic strength and repository conditions on plutonium solubilities in WIPP brines, showing that even with the uncertainties of the model parameters, the extremely reducing conditions at the WIPP will be well within the stability field of the Pu(III) solid phase.

6. Conclusions

Our review of the available experimental data as well as geochemical modeling results demonstrate that post-closure WIPP repository conditions will be extremely reducing due to multiple geochemical and physical processes. Metallic iron and the associated anoxic corrosion products are likely to facilitate plutonium reduction to Pu(III) solid in equilibrium with Pu(III) aqueous species. Organic ligands have the potential to affect plutonium oxidation states, though the low inventory of organic ligands makes them unlikely to have a major influence on plutonium oxidation states or solid phase solubilities. The effects of microbial processes on plutonium oxidation states in WIPP brines are uncertain, but if significant microbial activity occurs in the WIPP repository environment, our review of experiments conducted in low-ionic-strength environments indicate that microbial activity will also promote plutonium reduction. At the high total gas pressures in the WIPP repository necessary for release of brine (8 MPa–15 MPa) and high repository P_{H2}, the stability field of water expands to lower redox conditions, making the existence of Pu(III) solids even more likely. Finally, recent $Pu(OH)_3$(am) and PuO_2(nc,hyd) solubility investigations have shown that Pu(III) solids are likely to be stable within the stability field of water at 0.1 MPa (Cho et al., 2016; Tasi et al., 2018a).

The available evidence shows that in a bedded salt repository such as the WIPP, the rock mechanics of the repository, waste inventory, and brine intrusion are inextricably linked with the geochemistry, promoting extremely reducing conditions through increased repository P_{H2} and the presence of metallic iron, ferrous iron hydroxide, and magnetite that will favor highly reduced plutonium solids and aqueous species.

Experimental results obtained since initial WIPP certification in 1998 strongly indicate that Pu(III) solids and aqueous species are stable over a pe range wider than previously understood. Our model results suggest that plutonium solubilities in WIPP brines should be represented by dissolution of $Pu(OH)_3$(am) to form Pu(III) aqueous species. Using $Pu(OH)_3$(am) to represent the solubility of plutonium in WIPP likely would result in higher mean dissolved plutonium concentrations than if the formation of Pu(IV) solids is assumed. The assumption of plutonium solubility control by Pu(III) solid provides a conservative, but also realistic, upper limit to the dissolved plutonium concentration that may be released to the ground surface in the event of a drilling intrusion. There is uncertainty associated with the plutonium concentrations calculated using the ThermoChimie database, because the SIT approach is not optimized for the high ionic strengths observed in WIPP brines. Further experimental evaluation of the formation of Pu(III) solids at extremely low pe values as well as the influence of species such as borate on +III actinide solubilities in high-ionic-strength, alkaline solutions, will lead to the development of a more robust Pitzer database for ionic strength correction and will further reduce the uncertainty associated with the calculated Pu(III) solids solubilities in WIPP brines.

Our evaluation of WIPP redox under conditions necessary for a brine release to the surface has shown that extremely reducing conditions, including the presence of metallic iron, $Fe(OH)_2$(cr), and/or magnetite will lead to plutonium solubility control by Pu(III) solid. While redox conditions in other deep geologic repositories may differ from those in the long-term WIPP repository because of differing depths, host rocks, waste forms, engineered barriers, and other factors, our work has identified some important considerations that are needed to estimate potential dissolved plutonium concentrations over regulatory and geologic timescales. Prediction of the effects of redox conditions on actinide solubilities and potential releases will require detailed site-specific evaluation of the unique physical and chemical characteristics at each repository site.

Declaration of competing interest

The authors declare that they have no known competing financial interests or personal relationships that could have appeared to influence the work reported in this paper.

Acknowledgements

The authors thank John J. Mahoney, Charles Wilson, Stephen Marschke, Ingrid Rosencrantz, Daniel Schultheisz, and the three anonymous reviewers for their technical reviews, as well as Robin Kemper for editorial review of this manuscript. The research described in this manuscript has been funded wholly or in part by the United States Environmental Protection Agency Contract EP-D-10-042 to SC&A Inc. The findings and conclusions in this report are those of the authors and do not necessarily represent the views of the funding agency.

Appendix A. Supplementary data

Supplementary data to this article can be found online at https://doi.org/10.1016/j.apgeochem.2020.104561.

References

Allard, B., Kipatsi, H., Liljenzin, J.O., 1980. Expected species of uranium, neptunium and plutonium in neutral aqueous solutions. J. Inorg. Nucl. Chem. 42, 1015–1027. https://doi.org/10.1016/0022-1902(80)80394-0.

AlMahamid, I., Becraft, K.A., Hakem, N.L., Gatti, R.C., Nitsche, H., 1996. Stability of various plutonium valence states in the presence of NTA and EDTA. Radiochim. Acta 74, 129–134. https://doi.org/10.1524/ract.1996.74.special-issue.129.

Altmaier, M., Geckeis, H., 2011. Plutonium and actinide chemistry in saline solutions. Plutonium Futur. Actinide Res. Q. 2, 29–32. Retrieved from https://www.lanl.gov/discover/publications/actinide-research-quarterly/index.php.

Altmaier, M., Neck, V., Lützenkirchen, J., Fanghänel, T., 2009. Solubility of plutonium in $MgCl_2$ and $CaCl_2$ solutions in contact with metallic iron. Radiochim. Acta 97, 187–192. https://doi.org/10.1524/ract.2009.1593.

André, C., Choppin, G.R., 2000. Reduction of Pu(V) by humic acid. Radiochim. Acta 88, 613–618. https://doi.org/10.1524/ract.2000.88.9-11.613.

Baes, C.F., Mesmer, R.E., 1976. The Hydrolysis of Cations. John Wiley & Sons, Toronto.

Banik, N., 2006. Speciation of Tetravalent Plutonium in Contact with Humic Substances and Kaolinite under Environmental Conditions. PhD thesis. Johannes Gutenberg-University Mainz. Retrieved from https://publications.ub.uni-mainz.de/theses/volltexte/2006/1182/pdf/1182.pdf.

Bolton, H., Rai, D., Xun, L., 2006. Biotransformation of Pu-EDTA: Implications to Pu Immobilization. DOE-BER Environmental Remediation Sciences Project #1010283, Richland, WA. https://doi.org/10.2172/895876.

Borkowski, M., Richmann, M., Reed, D.T., Xiong, Y., 2010. Complexation of Nd(III) with tetraborate ion and its effect on actinide(III) solubility in WIPP brine. Radiochim. Acta 98 (9–11). https://doi.org/10.1524/ract.2010.1756.

Boukhalfa, H., Reilly, S., Smith, W., Neu, M., 2003. Stability and redox behavior of plutonium-EDTA and mixed Pu(IV)-EDTA-L (L= hydroxide, carbonate, citrate) complexes. In: Jarvinen, G.D. (Ed.), Plutonium Futures – the Science, Third Topical Conference on Plutonium and Actinides, AIP Conf. Proc, vol. 673, pp. 238–240. https://doi.org/10.1063/1.1594618.

Boukhalfa, H., Reilly, S., Smith, W., Neu, M., 2004. EDTA and mixed-ligand complexes of tetravalent and trivalent plutonium. Inorg. Chem. 43, 5816–5823. https://doi.org/10.1021/ic035484p.

Boukhalfa, H., Icopini, G.A., Reilly, S.D., Neu, M.P., 2007. Plutonium(IV) reduction by the metal-reducing bacteria *Geobacter metallireducens* GS15 and *Shewanella oneidensis* MR1. Appl. Environ. Microbiol. 73, 5897–5903. https://doi.org/10.1128/aem.00747-07.

Brush, L.H., Domski, P.S., 2013. Prediction of Baseline Actinide Solubilities for the WIPP CRA-2014 PA. Sandia National Laboratories. ERMS 559138. Retrieved from https://www.wipp.energy.gov/library/cra/CRA-2014/References/authorFiles/Brush_L_H_and_P_Domski.htm.

Brush, L.H., Domski, P.S., 2013. Calculation of Organic Ligand Concentrations for the WIPP CRA-2014 PA. Sandia National Laboratories, Carlsbad, New Mexico. ERMS 559005. Retrieved from https://www.wipp.energy.gov/library/cra/CRA-2014/References/authorFiles/Brush_L_H_and_P_Domski.htm.

Capdevila, H., Vitorge, P., 1998. Solubility product of $Pu(OH)_4$(am). Radiochim. Acta 82, 11–16. https://doi.org/10.1524/ract.1998.82.special-issue.11.

Cho, H.-R., Youn, Y.-S., Jung, E.C., Cha, W., 2016. Hydrolysis of trivalent plutonium and solubility of $Pu(OH)_3$(am) under electrolytic reducing conditions. Dalton Trans. 45, 19449–19457. https://doi.org/10.1039/c6dt03992h.

Choppin, G.R., 1991. Redox speciation of plutonium in natural waters. J. Radioanal. Nucl. Chem. Artic. 147, 109–116. https://doi.org/10.1007/bf02039572.

Congress, U.S., 1996. Public Law 102-579. Waste Isolation Pilot Plant Land Withdrawal Act of 1992, as Amended by Public Law 104-201, 1996. Retrieved from. https://wipp.energy.gov/library/CRA/CRA%202019/T%20-%20W/USC%20%201996%20%20LWA%20Public%20Law%20102-579.pdf.

Ding, M., Conca, J.L., Den Auwer, C., Gabitov, R.I., Hess, N.J., Paviet-Hartmann, P., Palmer, P.D., LoPresti, V., Conradson, S.D., 2006. Chemical speciation of heterogeneously reduced Pu in synthetic brines. Radiochim. Acta 94, 249–259. https://doi.org/10.1524/ract.2006.94.5.249.

DOE (U.S. Department of Energy), 2014. Title 40 CFR Part 191 Subparts B and C Compliance Recertification Application for the Waste Isolation Pilot Plant. U.S. Department of Energy Carlsbad Field Office. March 2014. Retrieved from https://www.wipp.energy.gov/library/CRA/CRA-2014.html.

Emmerich, M., Bhansali, A., Lösekann-Behrens, T., Schröder, C., Kappler, A., Behrens, S., 2012. Abundance, distribution, and activity of Fe(II)-oxidizing and Fe(III)-reducing microorganisms in hypersaline sediments of Lake Kasin, Southern Russia. Appl. Environ. Microbiol. 78, 4386–4399. https://doi.org/10.1128/aem.07637-11.

EPA (U.S. Environmental Protection Agency), 2017. Technical Support Document for Section 194.24: Evaluation of the Compliance Recertification Actinide Source Term, Gas Generation, Backfill Efficacy, Water Balance and Culebra Dolomite Distribution Coefficient Values. Office of Radiation and Indoor Air. Docket No. EPA-HQ-OAR-2014-0609, June 2017. Retrieved from. https://wipp.energy.gov/.

Felmy, A.R., Rai, D., Schramke, J.A., Ryan, J.L., 1989. The solubility of plutonium hydroxide in dilute solution and in high-ionic-strength chloride brines. Radiochim. Acta 48, 29–35. https://doi.org/10.1524/ract.1989.48.12.29.

Felmy, A.R., Moore, D.A., Rosso, K.M., Qafoku, O., Rai, D., Buck, E.C., Ilton, E.S., 2011. Heterogeneous reduction of PuO_2 with Fe(II): importance of the Fe(III) reaction product. Environ. Sci. Technol. 45, 3952–3958. https://doi.org/10.1021/es104212g.

Felmy, A.R., Moore, D.A., Pearce, C.I., Conradson, S.D., Qafoku, O., Buck, E.C., Rosso, K.M., Ilton, E.S., 2012. Controls on soluble Pu concentrations in PuO_2/magnetite suspensions. Environ. Sci. Technol. 46, 11610–11617. https://doi.org/10.1021/es3028956.

Francis, A.J., Dodge, C.J., Ohnuki, T., 2007. Microbial transformations of plutonium. J. Nucl. Radiochem. Sci. 8, 121–126. https://doi.org/10.14494/jnrs2000.8.121.

Fujiwara, K., Yamana, H., Fujii, T., Moriyama, H., 2001. Solubility product of plutonium hydrous oxide. J. Nucl. Fuel Cycle Environ. 7, 17–23. Retrieved from https://nuce.aesj.or.jp/jnuce/vol7/Jnuce-Vol7-1-p17-24.pdf.

Gaona, S., Montoya, V., Colás, E., Grivé, M., Duro, L., 2008. Review of the complexation of tetravalent actinides by ISA and gluconate under alkaline to hyperalkaline conditions. J. Contam. Hydrol. 102, 217–227. https://doi.org/10.1016/j.jconhyd.2008.09.017.

Giffaut, E., Grivé, M., Blanc, P., Vieillard, P., Colàs, E., Gailhanou, H., Gaboreau, S., Marty, N., Madé, B., Duro, L., 2014. Andra thermodynamic database for performance

assessment: ThermoChimie. Appl. Geochem. 49, 225–236. https://doi.org/10.1016/j.apgeochem.2014.05.007.
Grenthe, I., Mompean, F., Spahiu, K., Wanner, H., 2013. Guidelines for the Extrapolation to Zero Ionic Strength. OECD Nuclear Energy Agency, Data Bank. TDB-2, Issy-les-Moulineaux, France. Retrieved from https://www.oecd-nea.org/dbtdb/guidelines/tdb2.pdf.
Guillaumont, R., Fanghänel, T., Neck, V., Fuger, J., Palmer, D.A., Grenthe, I., Rand, M.H., 2003. Update on the Chemical Thermodynamics of Uranium, Neptunium, Plutonium, Americium and Technetium. OECD Nuclear Energy Agency Data Bank. OECD Publications, Issy-les-Moulineaux, France. Retrieved from https://www.oecd-nea.org/dbtdb/pubs/vol5-update-combo.pdf.
Hinz, K., Altmaier, M., Gaona, X., Rabung, T., Schild, D., Richmann, M., Reed, D.T., Alekseev, E.V., Geckeis, H., 2015. Interaction of Nd(III) and Cm(III) with borate in dilute to concentrated alkaline NaCl, $MgCL_2$ and $CaCL_2$ solutions: solubility and TRLFS studies. New J. Chem. 39, 849–859. https://doi.org/10.1039/c4nj01203h.
Icopini, G.A., Lack, J.G., Hersman, L.E., Neu, M.P., Boukhalfa, H., 2009. Plutonium(V/VI) reduction by the metal-reducing bacteria *Geobacter metallireducens* GS-15 and *Shewanella oneidensis* MR-1. Appl. Environ. Microbiol. 75, 3641–3647. https://doi.org/10.1128/aem.00022-09.
Kelm, M., Pashalidis, I., Kim, J.I., 1999. Spectroscopic investigation on the formation of hypochlorite by alpha radiolysis in concentrated NaCl solutions. Appl. Radiat. Isot. 51, 637–642. https://doi.org/10.1016/s0969-8043(99)00113-x.
Kim, S., Marrs, C., Nemer, M., Je-Hun Jang, J., 2017. Solubility model for ferrous iron hydroxide, hibbingite, siderite, and chukanovite in high saline solutions of sodium chloride, sodium sulfate, and sodium carbonate. ACS Earth Space Chem. 1, 647–663. https://doi.org/10.1021/acsearthspacechem.7b00065.
Kirsch, R., Fellhauer, D., Altmaier, M., Neck, V., Rossberg, A., Charlet, L., Scheinost, A.C., 2010. Reaction of Pu(III) and Pu(V) with magnetite and mackinawite: a XANES/EXAFS investigation. Geochem. Cosmochim. Acta 74 (Suppl. l), 11–520. Retrieved from https://goldschmidtabstracts.info/abstracts/abstractView?id=2010002428.
Kirsch, R., Fellhauer, D., Altmaier, M., Neck, V., Rossberg, A., Fanghänel, T., Charlet, L., Scheinost, A.C., 2011. Oxidation state and local structure of plutonium reacted with magnetite, mackinawite and chukanovite. Environ. Sci. Technol. 45, 7267–7274. https://doi.org/10.1021/es200645a.
Knopp, R., Neck, V., Kim, J.I., 1999. Solubility, hydrolysis and colloid formation of plutonium(IV). Radiochim. Acta 86, 101–108. https://doi.org/10.1524/ract.1999.86.34.101.
Lemire, R.J., Garisto, F., 1989. The Solubility of U, Np, Pu, Th and Tc in a Geological Disposal Vault for used Nuclear Fuel. Whiteshell Nuclear Research Establishment, Atomic Energy of Canada Ltd., AECL–10009. Retrieved from https://inis.iaea.org/search/search.aspx?orig_q=RN:23037160.
Lemire, R.J., Fuger, J., Nitsche, H., Potter, P., Rand, M.H., Rydberg, J., Pahiu, K., Sullivan, J.C., Ullman, W.J., Vitorge, P., Wanner, H., 2001. Chemical Thermodynamics of Neptunium and Plutonium. Chemical Thermodynamics 4. OECD Nuclear Energy Agency Data Bank, Eds. OECD Publications, Issy-les-Moulineaux, France. Retrieved from https://www.oecd-nea.org/dbtdb/pubs/vol4-neptunium-plutonium.pdf.
Lovley, D.R., Chapelle, F.H., 1995. Deep subsurface microbial processes. Rev. Geophys. 33 (3), 365–381. https://doi.org/10.1029/95rg01305.
Marquardt, C.M., Seibert, A., Artinger, R., Denecke, M.A., Kuczewski, B., Schild, D., Fanghänel, T., 2004. The redox behaviour of plutonium in humic rich groundwater. Radiochim. Acta 92, 617–623. https://doi.org/10.1524/ract.92.9.617.55007.
Marquardt, C.M., Banik, N.L., Shcherbina, N., Geckeis, H., 2008. Redox behavior of plutonium and neptunium in aqueous solution containing humic substances or hydroquinone. In: NRC7 – Seventh International Conference on Nuclear and Radiochemistry. Hungary, August 24 – 28, 2008. Retrieved from https://www.researchgate.net/publication/238090717_Redox_behavior_of_Plutonium_and_Neptunium_in_aqueous_solution_containing_humic_substances_or_Hydroquinone.
Molecke, M.A., 1980. Gas generation from transuranic waste degradation. In: Northrup, C.J.M. (Ed.), Scientific Basis for Nuclear Waste Management, vol. 2. Springer, Boston, pp. 569–575. https://doi.org/10.1007/978-1-4684-3839-0_68.
NASEM (National Academies of Sciences, Engineering, and Medicine), 2018. Disposal of Surplus Plutonium at the Waste Isolation Pilot Plant: Interim Report. The National Academies Press, Washington, DC. https://doi.org/10.17226/25272.
NEA (Nuclear Energy Agency), 2018. Microbial Influence on the Performance of Subsurface Salt-Based Radioactive Waste Repositories. Organisation for Economic Co-operation and Development. Retrieved from http://www.oecd.org/publications/microbial-influence-on-the-performance-of-subsurface-salt-based-radioactive-waste-repositories-9789264303133-en.htm.
Neck, V., Altmaier, M., Fanghänel, T., 2007. Solubility of plutonium hydroxides/hydrous oxides under reducing conditions and in the presence of oxygen. Compt. Rendus Chem. 10, 959–977. https://doi.org/10.1016/j.crci.2007.02.011.
Nemer, M.B., Xiong, Y., Ismail, A.E., Je-Hun Jang, J., 2011. Solubility of $Fe_2(OH)_3Cl$ (pure-iron end-member of hibbingite) in NaCl and Na_2SO_4 brines. Chem. Geol. 280, 26–32. https://doi.org/10.1016/j.chemgeo.2010.10.003.
O'Donnell, J.H., 1991. Chemistry of radiation degradation of polymers. In: Clough, R.L., Shalaby, S.W. (Eds.), Radiation Effects on Polymers. ACS Symposium Series, vol. 475. American Chemical Society, Washington, DC, pp. 402–413. https://doi.org/10.1021/bk-1991-0475.ch024.
Parkhurst, D.L., Appelo, C.A.J., 2013. Description of input and examples for PHREEQC version 3—a computer program for speciation, batch-reaction, one-dimensional transport, and inverse geochemical calculations. In: U.S. Geological Survey Techniques and Methods, Book 6, Chapter A43. https://doi.org/10.3133/tm6a43.
Pavasars, I., Hagberg, J., Borén, H., Allard, B., 2003. Alkaline degradation of cellulose: mechanisms and kinetics. J. Polym. Environ. 11, 39–47. https://doi.org/10.1023/A:1024267704794.
Plymale, A.E., Bailey, V.L., Fredrickson, J.K., Heald, S.M., Buck, E.C., Shi, L., Wang, Z., Resch, C.T., Moore, D.A., Bolton, H., 2012. Biotic and abiotic reduction and solubilization of $Pu(IV)O_2{\bullet}xH_2O$(am) as affected by anthraquinone-2,6-disulfonate (AQDS) and ethylenediaminetetraacetate (EDTA). Environ. Sci. Technol. 46, 2132–2140. https://doi.org/10.1021/es2030752.
Popielak, R.S., Beauheim, R.L., Black, S.R., Coons, W.E., Ellingson, C.T., Olsen, R.L., 1983. Brine Reservoirs in the Castile Formation, Waste Isolation Pilot Plant Project, Southeastern New Mexico. D'Appolonia Consulting Engineers, Albuquerque, New Mexico. Retrieved from https://www.wipp.energy.gov/library/cra/CRA-2014/References/Others/Popielak_etal_1983_Brine_Reservoirs_in_the_Castile_Formation_WIPP_ERMS242085.pdf.
Rai, D., 1984. Solubility product of Pu(IV) hydrous oxide and equilibrium constants of Pu(IV)/Pu(V), Pu(IV)/Pu(VI), and Pu(V)/Pu(VI) couples. Radiochim. Acta 35, 97–106. https://doi.org/10.1524/ract.1984.35.2.97.
Rai, D., Strickert, R.G., Moore, D.A., Ryan, J.L., 1983. Am(III) hydrolysis constants and solubility of Am(III) hydroxide. Radiochim. Acta 33, 201–206. https://doi.org/10.1524/ract.1983.33.4.201.
Rai, D., Gorby, Y.A., Fredrickson, J.K., Moore, D.A., Yui, M., 2002. Reductive dissolution of PuO_2(am): The effect of Fe(II) and hydroquinone. J. Solut. Chem. 31, 433–453. https://doi.org/10.1023/A:1020200911842.
Rai, D., Moore, D., Rosso, K., Felmy, A., Bolton, H., 2008. Environmental mobility of Pu(IV) in the presence of ethylenediaminetetraacetic acid: myth or reality? J. Solut. Chem. 37, 957–986. https://doi.org/10.1007/s10953-008-9282-2.
Reed, D.T., Wygmans, D.G., Aase, S.B., Banaszak, J.E., 1998a. Reduction of Np(VI) and Pu(VI) by organic chelating agents. Radiochim. Acta 82, 109–114. https://doi.org/10.1524/ract.1998.82.special-issue.109.
Reed, D.T., Molecke, M.A., 1993. Generation of Volatile Organic Compounds by Alpha Particle Degradation of WIPP Plastic and Rubber Material. Argonne National Laboratory, Argonne, Illinois. ANL/CMT/CP-79852 https://digital.library.unt.edu/ark:/67531/metadc1273059/. Retrieved from.
Reed, D.T., Hoh, J., Emery, J., Hobbs, D., 1992. Radiolytic gas production in the alpha particle degradation of plastics. In: Proceeding of Waste Management, vol. 92, pp. 1081–1086. Retrieved from https://inis.iaea.org/search/search.aspx?orig_q=RN:23062470.
Reed, D.T., Wygmans, D.G., Richmann, M.K., 1996. Stability of Pu(VI), Np(VI), and U(VI) in Simulated WIPP Brine. Argonne National Laboratory Interim Report. Retrieved from https://www.wipp.energy.gov/library/CRA/2009_CRA/references/Others/Reed_Wygmans_Richmann_Actinide_Stability_Solubility.pdf.
Reed, D.T., Hoh, J., Emery, J., Okajima, S., Krause, T., 1998b. Gas Production Due to Alpha Particle Degradation of Polyethylene and Polyvinylchloride. Argonne National Laboratory ANL-97/7-97/7, Argonne, Illinois. https://doi.org/10.2172/303944.
Reed, D.T., Lucchini, J.F., Aase, S.B., Kropf, A.J., 2006. Reduction of plutonium (VI) in brine under subsurface conditions. Radiochim. Acta 94, 591–597. https://doi.org/10.1524/ract.2006.94.9-11.591.
Reed, D.T., Lucchini, J.F., Borkowski, M., Richmann, M.K., 2010. Reduction of Higher Valent Plutonium by Iron under Waste Isolation Pilot Plant (WIPP)-Relevant Conditions: Data Summary and Recommendations. LCO-ACP-09, LANL/ACRSP Report. Los Alamos National Laboratory, Los Alamos, NM. Retrieved from https://www.wipp.energy.gov/library/cra/CRA-2014/References/authorFiles/Reed_DT_J-F_Lucchini_M_Borkowski_and_MK_Richmann.htm.
Reed, D.R., Borkowski, M., Swanson, J., Richmann, M., Khaing, H., Lucchini, J.F., Ams, D., 2011. Redox-controlling processes for multivalent metals and actinides in the WIPP. Redox Phenomena Controlling Systems. In: Altmaier, M., Kienzler, B., Duro, L., Grivé, M., Montoya, V. (Eds.), 3rd Annual Workshop Proceedings, 7th EC Recosy Cooperative Project. Karlsruhe Institute for Technology. March 2011. Retrieved from https://wipp.energy.gov/library/CRA/CRA-2014/References/Others/Reed_etal_2011_Redox_controlling_processes_of_multivalent_metals_and_actinides_in_the_WIPP_Recoxy.pdf.
Renshaw, J.C., Law, N., Geissler, A., Livens, F.R., Lloyd, J.R., 2009. Impact of the Fe(III)-reducing bacteria *Geobacter sulfurreducens* and *Shewanella oneidensis* on the speciation of plutonium. Biogeochemistry (Dordr.) 94, 191–196. https://doi.org/10.1007/s10533-009-9318-8.
Rusin, P.A., Quintana, L., Brainard, J.R., Strietelmeir, B.A., Tait, C.D., Ekberg, S.A., Palmer, P.D., Newton, T.W., Clark, D.L., 1994. Solubilization of plutonium hydrous oxide by iron-reducing bacteria. Environ. Sci. Technol. 28, 1686–1690. https://doi.org/10.1021/es00058a021.
Saheb, M., Neff, D., Demory, J., Foy, E., Dillman, P., 2010. Characterisation of corrosion layers formed on ferrous archaeological artefacts buried in anoxic media. Corrosion Eng. Sci. Technol. 45, 381–387. https://doi.org/10.1179/147842210X12772898886889.
Schott, J., Kretzschmar, J., Acker, M., Eidner, S., Kumke, M.U., Drobot, B., Barkleit, A., Taut, S., Brendler, V., Stumpf, T., 2014. Formation of a Eu(III) borate solid species from a weak Eu(III) borate complex in aqueous solution. Dalton Trans. 43, 11516–11528. https://doi.org/10.1039/c4dt00843j.
Selwyn, L., 2004. Overview of archaeological iron: the corrosion problem, key factors affecting treatment, and gaps in current knowledge. In: Ashton, J., Hallam, D. (Eds.), Metal 04: Proceedings of the International Conference on Metals Conservation. National Museum of Australia, Canberra, pp. 294–306. Retrieved from https://www.nma.gov.au/_data/assets/pdf_file/0008/346058/NMA_metals_s3_p06_overview_archaeological_iron.pdf.
Smart, N.R., Blackwood, D.J., Werme, L., 2001. The Anaerobic Corrosion of Carbon Steel and Cast Iron in Artificial Groundwaters. SKB, Swedish Nuclear Fuel and Waste Management Co., Stockholm, Sweden. Retrieved from https://www.skb.com/publications/?articleId=tr-01-22&title&author&publication_search&type=0&language=0&start_year&end_year&orderby=bibas_date&order=desc.

Snider, A.C., 2003. Verification of the Definition of Generic Weep Brine and the Development of a Recipe for This Brine. Sandia National Laboratories, Carlsbad, New Mexico. Retrieved from https://www.semanticscholar.org/paper/Verification-of-the-Definition-of-Generic-Weep-and-Snider/a3c60d537b89237ac5f827fd3b6f4ac5867ed4e4.

Swanson, J.S., 2013. Microbial characterization of halite and groundwater samples from the WIPP0. Los Alamos National Laboratory LA-UR-26280, p. 26280. https://doi.org/10.2172/1089877.

Swedin, J., 2019. Report 2019. Overview of Eight Countries–Status April 2019, vol. 1. The Swedish National Council for Nuclear Waste. Retrieved from https://www.karnavfallsradet.se/en/report-20191-overview-of-eight-countries-status-april-2019.

Tasi, A., Gaona, X., Fellhauer, D., Böttle, M., Rothe, J., Dardenne, K., Schild, D., Grivé, M., Colàs, E., Bruno, J., Källström, K., Altmaier, M., Geckeis, H., 2018a. Redox behavior and solubility of plutonium under alkaline, reducing conditions. Radiochim. Acta 106, 259–279. https://doi.org/10.1515/ract-2017-2870.

Tasi, A., Gaona, X., Fellhauer, D., Böttle, M., Rothe, J., Dardenne, K., Polly, R., Grivé, M., Colàs, E., Bruno, J., Källström, K., Altmaier, M., Geckeis, H., 2018b. Thermodynamic description of the plutonium – α-D-isosaccharinic acid system I: solubility, complexation and redox behavior. Appl. Geochem. 98, 247–264. https://doi.org/10.1016/j.apgeochem.2018.04.014.

Telander, M.R., Westerman, R.E., 1997. Hydrogen Generation by Metal Corrosion in Simulated Waste Isolation Pilot Plant Environments. SAND96-2538, Prepared for Sandia National Laboratories, Albuquerque, New Mexico by Pacific Northwest. National Laboratory, Richland, Washington. https://doi.org/10.2172/461274.

Van Loon, L.R., Glaus, M.A., 1997. Review of the kinetics of alkaline degradation of cellulose in view of its relevance for safety assessment of radioactive waste repositories. J. Environ. Polym. Degrad. 5, 97–109. https://doi.org/10.1007/BF02763593.

Van Soest, G.D., 2018. Performance Assessment Inventory Report – 2018. Los Alamos National Laboratory Carlsbad Operations, INV-PA, 18, Revision 0, INV-1812-01-01.

Westerhoff, P., 2003. Reduction of nitrate, bromate, and chlorate by zero valent iron (Fe^0). J. Environ. Eng. 129, 10–16. https://doi.org/10.1061/(asce)0733-9372(2003)129:1(10).

Wolery, T.J., Xiong, Y.-L., Long, J.J., 2010. Verification and Validation Plan/Validation Document for EQ3/6 Version 8.0a for Actinide Chemistry, Revision 1, Document Version 8.20. Sandia National Laboratories, Carlsbad, New Mexico. Retrieved from https://wipp.energy.gov/library/CRA/CRA-2014/References/Others/Xiong_2011_WIPP_Verification_and_Validation_PlanValidation_Document_for_EQ36_Version_8_0a_ERMS555358.pdf.

Xia, Y., Rao, L., Rai, D., Felmy, A.R., 2001. Determining the distribution of Pu, Np, and U oxidation states in dilute NaCl and synthetic brine solutions. J. Radioanal. Nucl. Chem. 250, 27–37. https://doi.org/10.1023/A:1013203911522.